

FINAL PUBLISHABLE REPORT

Grant Agreement number 16ENV09
 Project short name MetroDECOM II
 Project full title In-situ metrology for decommissioning nuclear facilities

Project start date and duration:		1 st September 2017, 42 months
Coordinator: Peter Ivanov, Dr NPL		Tel: +44(0)20 8943 8598
Project website address: http://empir.npl.co.uk/metrodecom/		E-mail: peter.ivanov@npl.co.uk
Internal Funded Partners:	External Funded Partners	Unfunded Partners:
1. NPL, United Kingdom	9. ANDRA, France	N/A
2. CEA, France	10. EDF, France	
3. CIEMAT, Spain	11. JRC, Europe	
4. CMI, Czech Republic	12. LL, United Kingdom	
5. ENEA, Italy	13. MAGICS, Belgium	
6. LNE, France	14. NNL, United Kingdom	
7. PTB, Germany	15. NUVIA, Czech Republic	
8. VTT, Finland	16. TAU, Finland	
RMG1: CIEMAT, Spain (Employing organisation); FTMC, Lithuania (Guest working organisation)		
RMG2: CIEMAT, Spain (Employing organisation) ENEA, Italy (Guest working organisation)		



TABLE OF CONTENTS

1	Overview	3
2	Need	3
3	Objectives	3
4	Results	4
5.	Impact	33
6.	List of publications.....	35
7.	Contact details	35

1 Overview

This project addressed one of the most significant environmental challenges facing EU member states: ensuring the safe disposal of radioactive waste from decommissioning nuclear sites. The key to dealing with such wastes was quantifying the radioactivity content, so that decommissioning can be planned and implemented to minimise the risk to members of the public and the environment.

The project aimed to provide nuclear site operators with measurement techniques that can be used to measure radioactivity for planning decommissioning, for segregating and checking waste materials during demolition, and for monitoring the condition of waste packages in radioactive waste repositories.

The project objectives were successfully achieved and the project's final results have addressed significant measurement challenges in the nuclear decommissioning sector in terms of rapid and automated radiochemical destructive analysis of solid samples, remote gamma- and alpha-screening and mapping of contamination, materials characterisation and waste sentencing as well as monitoring of repository sites. Uptake and application of the novel methods and prototype instrumentation developed within the project will allow the user community to facilitate and accelerate the process of on-site radiological characterisation, ultimately leading to safer, cost efficient and environmentally friendly decommissioning of nuclear facilities.

2 Need

Previous to the start of the project, first-generation nuclear power plants and reprocessing facilities were coming to the end of their working lives. As per November 2020, a hundred nuclear power reactors have been shut down for decommissioned in the EU and most of the remaining 116 reactors plus fuel cycle facilities will also be in decommissioning by 2030.

The aim of the decommissioning process is to clear the site, while minimising the risk to the public and the environment from the hazardous waste arising. The cost of decommissioning and waste management in the EU is estimated to be in excess of 150 billion Euro.

The key to safe and cost-effective disposal of the waste is accurate characterisation – determining the physical, chemical, and radiological characteristics of the material. This enables nuclear site operators to plan the demolition process, assign the waste to the most cost-effective disposal route and then to monitor that the waste is being stored safely. The metrological challenge was that nuclear sites have been operating for many decades, so the disposition and quantities of hazardous materials were not well known. There was significant progress towards studies on the scientific bases of novel methods for material and waste characterisation within the frames of the previous EMRP projects ENV09 MetroRWM and ENV54 MetroDECOM. The present project built on these bases and focussed on bringing the techniques into use on nuclear sites and developing of robust and efficient procedures and instrumentation for radiological characterisation of decommissioning wastes and materials.

Regulatory bodies and international organisations have therefore carried out detailed studies of technical needs in the field. The common themes that have been raised were: (1) improvements in capability, (2) harmonisation and quality assurance, and (3) sharing knowledge. The improvements in capability that were required included rapid, on site measurements improving the accuracy and traceability of measurements of waste packages.

These needs were reflected in EU Council Directive 2011/70/EURATOM which focuses on encouraging technical co-operation to improve safe management of radioactive waste and highlights the importance of building public trust and confidence.

3 Objectives

The overall objective of this project was to establish a measurement infrastructure that is accepted and implemented by the nuclear industry for the measurement of radioactivity, temperature and stress needed for nuclear decommissioning.

The objectives of the project were:

1. To develop in situ methods for the rapid radionuclide characterisation of the different types of materials present on decommissioning sites. This includes the development of novel measurement techniques

that improve the mapping of contamination inside nuclear facilities and the determination of statistically valid and effective sampling methods.

2. To develop and implement traceable measurement systems and methods for waste pre-selection and free release to the environment. This includes the on-site validation of existing waste pre-selection and free release measurement systems and evidence of their traceability to primary standards.
3. To develop a validated waste repository acceptance characterisation system for use on site with very low and intermediate level radioactive waste (LLW and ILW). The system will include gamma scanning and passive neutron measurements and will be sensitive to fissile material.
4. To develop improved measurement systems and methods for monitoring radioactive waste repositories. This includes miniaturised, portable and rapidly deployable gas and water monitoring systems, improved water monitoring systems and systems for monitoring the temperature and strain of inside nuclear waste repositories for the long term. All the systems will be verified with on-site testing.
5. To facilitate the take up of the technology and measurement infrastructure developed in the project by nuclear decommissioning operators, measurement device producers, radiation protection regulators and standards developing organisations. In addition, to establish in collaboration with the end-user community a European network that will co-ordinate a measurement infrastructure for decommissioning nuclear facilities.

4 Results

4.1. Development and implementation of rapid methods for measuring the radioactivity content of materials on a nuclear site

In-situ measurement of radioactivity and dose levels are a key part of achieving safe and cost-effective decommissioning. Accurate on-site measurements reduce the amount of destructive analysis and material that must be transported off site for analysis, minimising procedural time, secondary waste and analyst time, thereby offering economic benefits for end users. As part of the metrology for rapid radionuclide characterisation of materials on decommissioning sites, a gamma camera protocol has been developed and validated at CEA against multiple gamma sources. The remote alpha contamination mapping method has been further developed by TAU to successfully achieved the required detection efficiency. A dose mapping array built with battery-operated compact, cheap wireless radiation detectors has been set up and validated by using various sources and in-situ measurements on a nuclear site.

4.1.1. Evaluation of the performance of a gamma camera

GAMPIX gamma camera, previously developed by CEA and industrialised by MIRION Technologies (CANBERRA) under the commercial name iPIX has been used by CEA in this study in combination with the novel Timepix counting chip hybridized to a 1 mm thick cadmium telluride (CdTe) semi-conductor to enable spectrometric measurements. Figure 1 shows GAMPIX gamma camera and its building blocks.

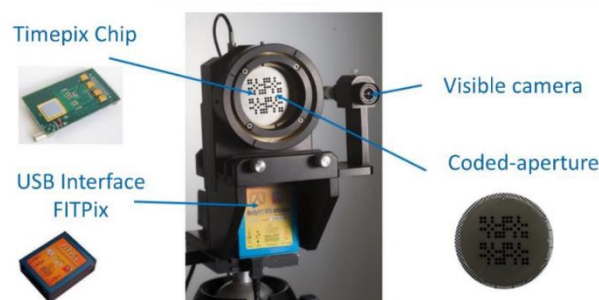


Figure 1. GAMPIX gamma camera and its building blocks: Timepix chip, USB Interface FITPix, visible camera, and MURA coded aperture.

To evaluate spectrometric performances of GAMPIX camera, the evolution of the energy resolution with the energy, and the relative error on the measured energy were investigated at CEA using a set of ^{241}Am , ^{152}Eu , ^{137}Cs , ^{133}Ba , ^{60}Co and ^{57}Co sources. The spectrometric performance of the gamma camera is presented on Figure 2, showing the evolution of the energy resolution with the energy of the incident photon on the left and the evolution of the relative error with the measured energy on the right.

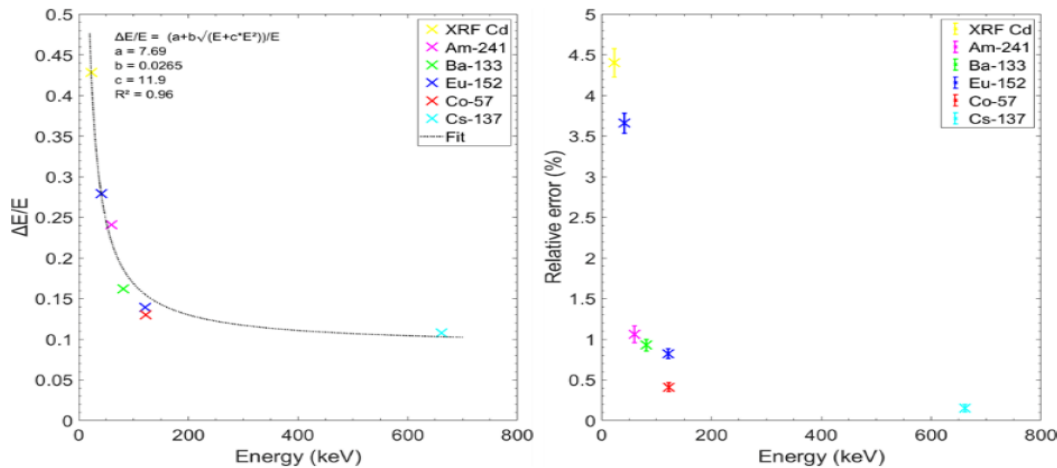


Figure 2. Spectrometric performances of GAMPIX: evolution of the energy resolution with the energy of the incident photon (left), and evolution of the relative error on the measured energy (right).

The energy resolution of GAMPIX is 15 % lower for photons with an energy above 100 keV, and the relative error is lower than 1.1 % for photons with an energy above 59.5 keV. The use of new generation pixelated chip Timepix3, developed by CERN, was found to allow a fine time sampling (25 ns) and significantly improves the spectrometric performances of the gamma camera. Timepix3 is a hybrid-pixel readout chip that can record simultaneously Time-Over-Threshold (ToT) and Time-Of-Arrival (ToA) in each pixel. The chip is designed to work in data-driven mode and is able to process up to 40 Mhits/cm²/s. Timepix3 consists in a matrix composed of 256x256 squared-shaped pixels with 55 μm pitch. For each measured event, the ToT gives access to the deposited energy, and the ToA to the time of interaction within the sensor.

In Timepix3, the energy deposited by an incident particle is measured using the Time over Threshold (ToT) method, which consists of measuring the time spent by a pulse voltage above a chosen threshold. The objective of the energy calibration is to convert the ToT values in energy values. The energy calibration per pixel of two Timepix3 detectors was performed. One of the detectors was hybridized with a 300 μm thick silicon (Si) semi-conductor, and the other was hybridized with a 1 mm thick cadmium telluride (CdTe) semi-conductor. The Timepix3 Si per pixel spectra of a ^{241}Am source and per pixel energy calibrated spectra are given in Figure 3.

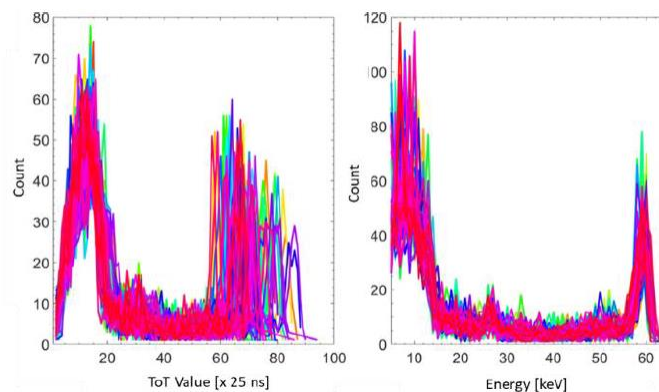


Figure 3. Timepix3 Si per pixel spectra of a ^{241}Am source showing per pixel ToT spectra (left) and per pixel energy calibrated spectra (right).

The energy calibration enabled defining the energy thresholds of Timepix3 Si and Timepix3 CdTe at 3.4 keV and 15 keV, respectively. The spectrometric performances of both detectors were evaluated by studying the evolution of both the energy resolution and the relative error, as a function of the energy. The results for Timepix3 Si show energy resolution of <10 % for photons with energy greater than 25 keV with relative error on measured energy of less than 0.5 %. Likewise, for Timepix3 CdTe the energy resolution was less than 10 % for photons with energy greater 100 keV.

4.1.2. Remote alpha-contamination mapping

Alpha emitting radionuclides are very difficult to measure in situ, due to the short range of the particles emitted. There have been some studies and prototype instruments to use the UV light emitted when nitrogen in the atmosphere is ionised, to detect the alpha-particles remotely. None of the instruments have previously proven to be sufficiently sensitive or suitable for use in a decommissioning environment. Therefore, the aim of this part of the project was to develop a model for remote alpha contamination mapping, followed by experimental studies to confirm the target sensitivity. The optical remote mapping of alpha contamination was performed by TAU using a Galilean style telescope and a photomultiplier tube (PMT) as a detector. The construction is based on a proof-of-concept design having a light collecting lens diameter of 10 cm and a specific wavelength filter stack in front of the detector. Figure 4 shows a schematic diagram of the arrangement and the picture of the instrument.

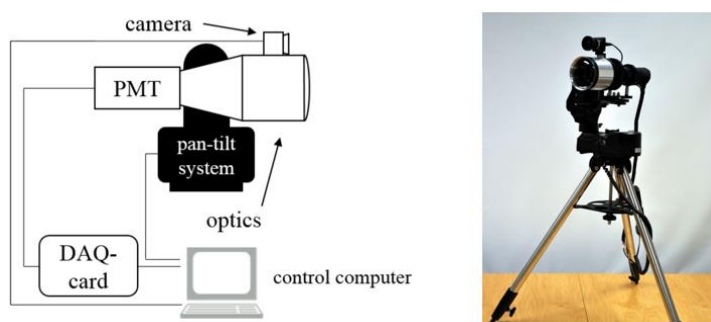


Figure 4. Schematic diagram of the PMT scanner setup (left) and photo of the prototype instrument (right).

The telescope optics was designed by TAU for indoor environments, where the lighting can be designed to be UV-free, e.g. using LED lighting. The selected PMT detector (H10682-210, Hamamatsu) has a quantum efficiency of approximately 30 % for the strongest radioluminescence peak at 337 nm wavelength. However, the PMT is also responsive to light at other wavelengths from 230 nm to 700 nm. Therefore, bandpass filters must be used to attenuate the unwanted wavelengths. A filter stack of three dielectric filters (3 x FF01-335/7-25, Semrock) was used to achieve the desired attenuation while still providing high transmittance at 337 nm. A small CMOS camera was placed on top of the telescope to give a grayscale view of the target area. The detected radioluminescence will then be colour coded on top of the grayscale photograph.

The PMT scanner sensitivity was enhanced by introducing a N₂/NO gas flush on the sample area. The flushing greatly enhances the deep UV luminescence at the 260 nm wavelength, which makes the method easy to utilize in any indoor lighting conditions. The PMT scanner instrument was modified with another filter/PMT setting to achieve deep-UV detection at 260 nm and solar-blind behaviour. The combination of deep-UV PMT (H11870-09, Hamamatsu) and efficient bandpass filtering (3 x FF01-260/16-25, Semrock) resulted the PMT scanner being effectively background free.

A minimum detectable activity of the PMT scanner instrument in comparison to ICCD camera method is shown in Figure 5. This data corresponds to normal room air conditions and UV free soft lighting (50 lux) by white LEDs. The target sensitivity of 10 kBq at the distance of 1 m is achieved with total image mapping time of about 10 minutes depending on a scanning mode and parameters. Longer total integration time naturally enhances the limit of detection.

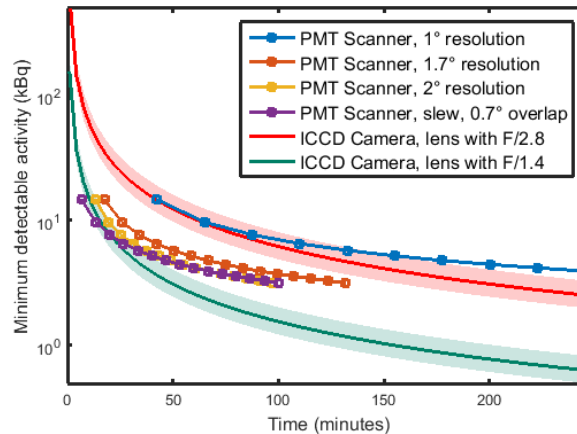


Figure 5. Minimum detectable activity plotted as a function of the total measurement time for PMT Scanner with three different resolutions with a measurement distance of 1 m. Data points of PMT Scanner curves begin from 1 s integration time per pixel and continue with 1 s increments.

It was shown that flushing the sample area with nitrogen gas containing trace amounts of nitric oxide, the deep UV radioluminescence can be greatly enhanced. The deep UV radioluminescence at the 220 – 280 nm wavelength is very well suited for practical applications as at that wavelength range has no disturbing background light from daylight or artificial lighting sources. Figure 6 shows radioluminescence mapping data collected with the PMT scanner with 30 s integration time per pixel. The sample in the experiment is a surface of natural uranium having a total surface alpha emission rate of about 1 kBq, which corresponds to activity per surface area of 40 Bq/cm².

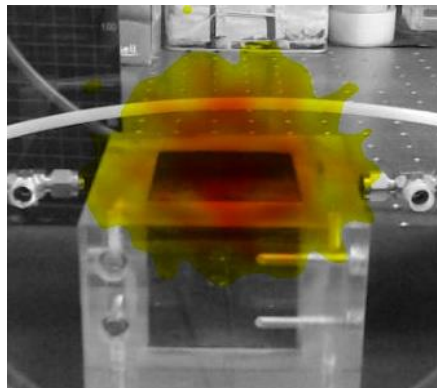


Figure 6. Radioluminescence mapping of natural uranium sample. The radioluminescence signal strength is colour coded in data post-processing on top of the grayscale photograph

By measuring a range of alpha sources at TAU, it was demonstrated that the method can still detect as low surface activity as 1.5 Bq/cm². These results open great application possibilities for alpha contamination imaging in gloveboxes and other closed chambers that can be flushed with nitrogen. Most importantly, the method can be utilized under normal lighting conditions without any modifications which makes it applicable for nuclear decommissioning applications.

4.1.3. Compact wireless radiation detectors for contamination and dose mapping

Measurement of the spatial distribution of dose rates is a useful tool in determining the disposition of radioactivity. At present, measurements are carried out by expensive dosimeters or gamma spectrometers that require manual operation. This project uses a novel setup representing a distributed network of compact sensors to determine the dose rate continuously as a function of location, using wireless transmission so they

can be installed easily in existing buildings and provide real-time dose maps. The high number of relatively cheap data points allows an optimised uncertainty of the initial mapping results in automated measurements. A distributed array of compact, wirelessly connected radiation detectors has been set up by MAGICS and used in the dose mapping measurements. Schematic view of the array and the wireless communication setup is given in Figure 7.

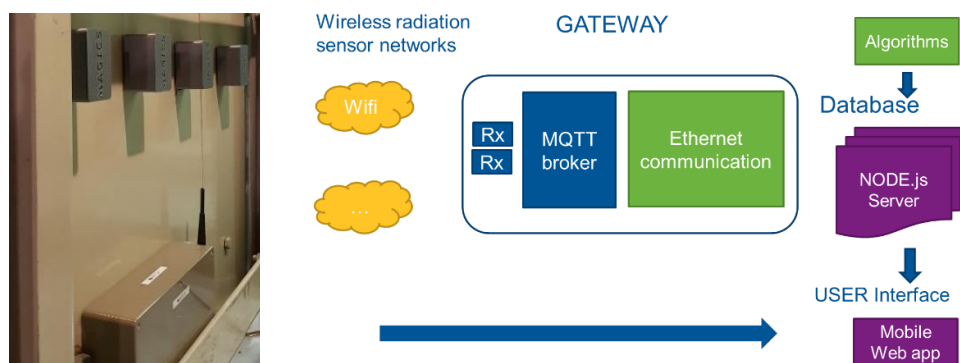


Figure 7. Schematic view of the detector array (left) and the wireless communication setup (right)

Dose-rate sensors have been commissioned and a validation study has been performed to verify the information in the data sheets of the selected low power radiation sensor. Five ^{137}Cs sources with activity ranging from 132 Bq to 23.1 kBq were used to determine the linearity. A random set of radiation sensors were selected to verify the linearity of the sensors. The datasheet indicated a variation of $\pm 15\%$ for a dose rate of $1\ \mu\text{Sv/h}$. The linearity for all sensors in terms of the R^2 value is good, with a value of greater than 0.998. Furthermore, a set of measurements has been performed to map the radiation dose around a real waste management facility in order to test and demonstrate the functionality of the sensor's platform and the results of which are given in Figure 8.



Figure 8. Measured radiation dose map at a radioactive waste management facility

Reconstruction of the radiation field based on the laboratory and in-situ measurement results has been investigated using different approaches such as theoretical, geostatistical and Bayesian inference. These results, together with the data from evaluation of the effect of the number of measurements indicate that the Bayesian inference method is the optimal choice to estimate the number of measurements points that can be removed in a mapping exercise. The basic geostatistical approach fails in reconstructing the radiation field when the number of measurement points are reduced. By comparison, Bayesian methods achieve effective reconstruction of the radiation field, especially for the high activity measurement points.

4.1.4. **Radiochemical characterisation procedures for ^{90}Sr , U and Pu isotopes, ^{41}Ca and ^{93}Zr in relevant matrices.**

Many radionuclides are not measurable using non-destructive techniques and require the development of robust, reproducible procedures, incorporating digestion of solid samples, chemical separation from interferences and measurement using radiometric or mass spectrometric techniques. The aim of this objective

was to develop robust, reproducible, automated sample preparation and measurement procedures for detection of decommissioning radionuclides in challenging sample matrices. Dissolution of >3 g concrete samples has been achieved using automated fusion, followed by multi-stage chemical and/or ICP-MS based separation procedures for U, Pu, ^{90}Sr , ^{41}Ca and ^{93}Zr . The procedure for simultaneous separation of U, Pu and ^{90}Sr has been successfully tested by NNL, using a semi-automated microfluidic radiochemistry system. The development of rapid and automated protocols offers benefits to end users through improved reproducibility, reduced analyst time, fewer resins and reagents and reduced secondary waste, which along with the decrease in procedural time contributes to reducing the cost of nuclear decommissioning.

4.1.4.1. Developing sample preparation protocols for digestion of decommissioning materials

The aim of this task was to modify procedures developed in the previous EMRP project ENV54 MetroDECOM to tolerate sample masses of >3 g compared to 0.5 - 1 g. The higher matrix content of such samples must be considered when developing radiochemical separation procedures. The starting point for the adjustment and optimisation of the sample preparation protocols was the set of procedures developed in EMRP project ENV54 MetroDECOM for concrete. PTB and NPL both investigated fusion-based dissolution with the aim of achieving a rapid analytical strategy and a sample that could be taken forward for radiochemical separation.

Automated fusion was performed using a single position Spex Katanax K1 Prime (PTB) and a 5-position Spex Katanax K2 prime (NPL). Digestions were carried out using 30 mL straight-walled 95 % Pt 5 % Au crucibles. For lithium borate fusion studies, the sample:flux ratio and furnace temperature conditions were optimised by measuring concrete samples from 1-5 g at 1 g intervals. Post-dissolution, 0.1 mL aliquots were taken and diluted to a total volume of 20 mL with 0.3 M HNO_3 and measured by ICP-MS (Agilent 8800 ICP-MS/MS). To assess the recovery of ^{41}Ca , stable ^{44}Ca was measured. Several other stable elements (Co, Sr, Ba and Eu) were also measured as analogues of radionuclides of interest to concrete (^{60}Co , ^{90}Sr , ^{133}Ba and ^{152}Eu). Blank concrete samples (1-5 g) prepared for the previous EMRP project ENV54 MetroDECOM were spiked with a multi-element solution and subjected to borate fusion dissolution. Aliquots of the dissolved samples were taken for measurement by ICP-MS/MS. For ^{93}Zr , the sample matrix of interest was stainless steel dissolved in concentrated nitric acid. The focus for this radionuclide was on radiochemical separation and sample dissolution of this material was not considered.

Lithium borate fusion for dissolution of 0.5-1 g concrete samples using a 50/50 mixture of lithium metaborate and lithium tetraborate at a sample:flux ratio of 1:4. At sample masses up to 5 g, dissolution was successful at a sample:flux ratio of 1:1.2 (e.g. 5 g sample and 6 g flux). The mass of lithium bromide non-wetting agent used was also increased to 0.3 g compared to 0.1 g for 0.5 g samples. The fusion temperature was increased, whilst the intensity and extent to which the samples were rocked was reduced to account for the high sample and flux masses (Table 1)

Table 1. Comparison of furnace operating conditions for original (0.5 g) and modified (3.0 g) procedures for borate fusion dissolution of concrete. *% of maximum rocking and pouring speed

Procedure	Original procedure (0.5 g)	Modified procedure (3 g)
Heating	Stage 1: 1000°C, 4 min Stage 2: 1020°C, 1 min	Stage 1: 1020°C, 5 min Stage 2: 1040°C, 1 min
Rocking	Stage 1: 90 %*, 20° Stage 2: 25 %, 5°	Stage 1: 20 %, 5° Stage 2: 20 %, 5°
Pouring	55 %, 120°	70 %, 130°

For sample sizes of 2-4 g, the count ratios for Ca relative to 1 g show good agreement (Figure 9).

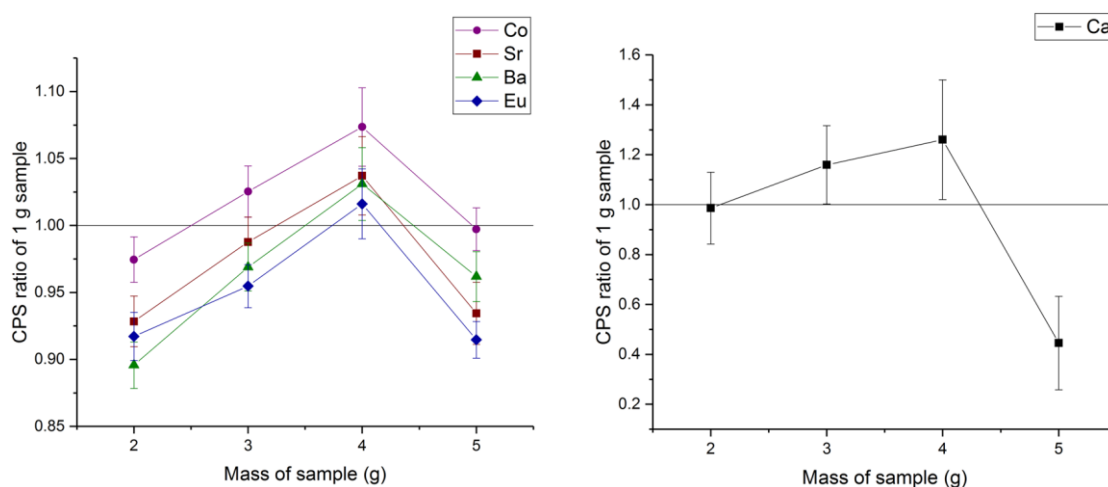


Figure 9. Count ratio of multiple elements for increasing sample mass compared to 1 g samples

The data is similar for other elements tested (Co, Sr, Ba and Eu). By comparison, the count ratio for 5 g samples was lower than expected. Possible reasons for this are that the sample/flux mixture did not successfully go completely into solution, or that there was some loss of analyte to the PEG precipitate. Despite this, the procedure developed successfully reached the project requirement to process at least 3 g of sample.

To overcome some of the difficulties derived from the presence of silicates in solution following borate fusion, it was decided to develop a sample treatment based on fusion using potassium fluoride (KF) as a flux. Fluoride fusions are used for the removal of silicon, the destruction of silicates and rare earth minerals, and the analysis of oxides of niobium, tantalum, titanium, and zirconium. Silicon is volatilized during this process, for which it results a very adequate for this type of analyses and was the approach selected.

A first sample treatment scheme was developed based on a fluoride fusion followed by a dissolution of the fused material with HNO_3 to allow the precipitation of fluorides, which leads to coprecipitation of all the analytes. The fluoride precipitation process was optimised by adjusting the pH value of the solution to pH 4 to achieve the quantitative precipitation of the analytes. The oxidation state adjustment of the actinides after fusion was also optimised in order to achieve its quantitative precipitation.

An important limitation of using KF as flux is the presence of fluoride in the final solution, which poses a problem for the subsequent analysis of many elements. In order to overcome this drawback, a second step was included following the KF fusion, which consisted of a second fusion using sodium carbonate as a flux to transform the fluorides into carbonates, which were precipitated in water.

The new scheme proved to be suitable for the treatment of mineral samples. The different tests showed that the procedure was reproducible and that it did not present any drawbacks of the previous schemes. The introduction of a new fusion step lengthened the whole process, but it still can be completed in less than 4 h, so it is suitable for the objectives of this project.

4.1.4.2. Optimising radiochemical separation protocol

The aim of this task was to develop radiochemical separation schemes focusing on simultaneous separation of U, Pu and ^{90}Sr , as well as customised procedures for ^{41}Ca and ^{93}Zr . These radionuclides were first investigated in the previous EMRP project ENV54 MetroDECOM, and in the present project procedures were modified to account for the higher matrix content associated with the elevated sample masses. In all cases, the procedures developed were divided into bulk matrix precipitation followed by radionuclide-specific extraction chromatography using resins developed by Triskem Internationalⁱ. In the case of ^{41}Ca and ^{93}Zr , consideration was also given to online separation using tandem ICP-MS/MS as a rapid alternative to offline chemical separation.

A separation set-up including stacked extraction chromatography cartridges connected to a vacuum box as shown in Figure 10 was used in all tests.



Figure 10. Stacked TEVA, UTEVA and Sr-resin cartridges for sample loading (left) and single cartridges for specific U, Pu and ^{90}Sr elution

The radiochemical procedure developed for U, Pu and ^{90}Sr separation was based on a tandem set-up of three cartridges with extraction chromatography resins ensuring selective retention of Pu(IV) by TEVA, uranium by UTEVA and strontium by Sr-resin.

TEVA cartridges were used for the extraction of plutonium using ^{242}Pu tracer as follows:

1. Loading the sample onto the resin in 3M HNO_3
2. Rinse with 3M HNO_3
3. Strip interferences from the resin:
 - a. Polonium (10 mL 8M HNO_3)
 - b. Thorium and Curium (20 mL 9M HCl)
4. Elute Pu with 20 mL of 1 % NH_3OHCl in 2M HCl

UTEVA cartridges were used for the extraction of uranium using ^{232}U as a tracer:

1. Loading the sample onto the resin in 3M HNO_3
2. Rinse with 3M HNO_3
3. Strip Th interference (5M HCl that was 0.05M with respect to $\text{H}_2\text{C}_2\text{O}_4$)
4. Elute U with 20mL of 0.01 M HCl

Electroplating of Pu and U was done according to the following procedure: a 2 mL solution of $\text{H}_2\text{SO}_4/\text{Na}_2\text{SO}_4$ (1:1) was added to each of the eluates and evaporated to dryness on a sand bath until no fumes were observed. Samples were then calcined over a Bunsen burner until the residue turned white. This residue was dissolved in an electrolyte solution and pH adjusted with HCl . Electroplating was done on stainless steel planchets for 1 h and planchets were rinsed with pure ethanol and left to dry on a hot plate for two hours before measurement. Activity concentration was measured by alpha-particle spectrometry using PIPS detectors (Canberra).

Sr-resin cartridges were used for the extraction of strontium using ^{85}Sr as a tracer:

1. Loading the sample onto the resin in 3 M HNO_3
2. Rinse with 8 M HNO_3
3. Elute Sr in 10 mL of 0.05 M HNO_3

Tracer recovery in this case was measured using high-resolution gamma spectrometry.

The recovery values achieved for the different elements varied and were influenced by the changes introduced in the sample dissolution scheme presented previously. The different chemical properties of the analytes often made it necessary to come to a compromise in order to achieve quantitative recovery of all radionuclides.

Pu was the element which presented the best results along the whole study, but it showed significant variability, ranging from 34 % to 100 %. In the case of U, high variability in the recovery values was observed along the whole study, ranging from 18 % to 64 %. Under the final analysis conditions, recovery reaches 36 %. The

recovery values of Sr were initially lower than 15 %, and only started improving once the fluoride precipitation conditions were optimised. Under the final analysis conditions, recovery reaches 37 %. In all three cases, the radiochemical recoveries achieved in the analysis of ^{90}Sr , U and Pu were good enough to allow accurate measurement of the radionuclides' activities.

Two single stage extraction chromatography set-ups were investigated for ^{41}Ca separation. The one based on Sr-resin achieved an average Ca recovery of 77 ± 3 % across the concrete samples tested and was preferred over the DGA-resin based method which showed 40 ± 11 % recovery. Furthermore, it was found that radiochemical separation with the Sr-resin is more time-efficient as the resin doesn't require an additional elution step to collect Ca.

Several tested resins showed potential for Zr/Nb separation. TEVA resin was the most promising candidate, with batch results suggesting Zr was not retained in 7-9 M HCl, whilst Nb was retained. Elution study tests were carried out at 7-9 M HCl using pre-packed 2 mL TEVA cartridges and a mixed stable Zr/Nb solution. Following a 10 mL load and 15 mL wash, the Zr recovery was 98 % in 7 M HCl, reducing to 86 % and <1 % in 8 M and 9 M HCl, respectively. Under all conditions, the Nb recovery was <1 %, suggesting that 7 M HCl represents the optimal conditions.

Furthermore, within the frames of a research mobility grant (RMG1, laboratory experiments were carried out towards the standardization of selected long-lived beta emitters of interest in decommissioning: Cl-36, Ca-41 and Tc-99. Using liquid scintillation counting, two methods based on the free parameter model have been applied for detection efficiency calculation: TDCR and CIEMAT/NIST calibration methods and uncertainties below 1% were achieved for the primary standardization of radionuclide solutions.

4.1.4.3. Testing separations in an automated radiochemical separation system

The aim of this activity was to test the radiochemical separation procedures using an automated radiochemistry system (NiV), based on a microfluidic device. There are a number of potential benefits to automated separation, including reduced operator dose and risk, fast and repeatable separations and resulting reduction in operating costs. The fully automated system incorporates a user interface, flow injection modules, a cartridge handling unit for configuring and manipulating the columns and a cartridge that can handle multiple chromatographic columns. Up to eight separations can be carried out simultaneously with minimal user interaction.

Unfortunately, a fully automated system was not available for these trials. Instead, all of the experimental data was obtained using a mock-up of the automated system which consisted of peristaltic pumps connected to a cartridge containing the resins of interest (**Error! Reference source not found.11**).

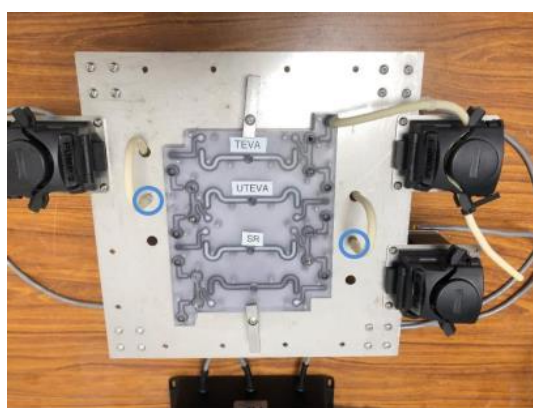


Figure 11. Semi-automated cartridge setup at NNL, containing TEVA, UTEVA and Sr-resin for simultaneous U, Pu and ^{90}Sr separation.

Of the separation schemes developed, the focus was on simultaneous separation of actinides (U, Pu) and ^{90}Sr using a stacked column arrangement developed by PTB. Two sets of trials were carried out at NNL. The first was on a simple dilute HNO_3 solution and the second was on a soil leachate based solution. In both cases, two successful trials were completed. Recoveries for the dilute HNO_3 trials are shown in Figure 12.

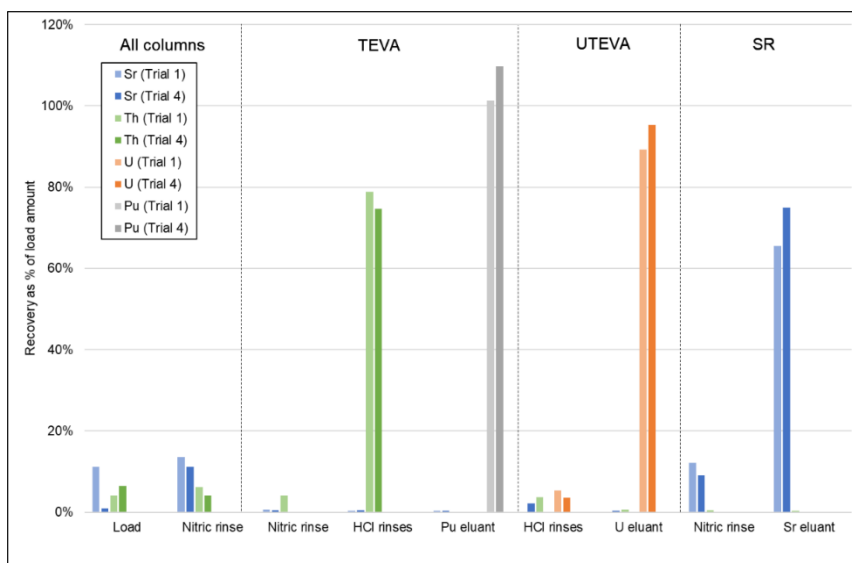


Figure 12. Recoveries for each collected fraction expressed as % of load amount for dilute HNO₃ trials.

Results show quantitative Pu recoveries and 89 % to 95 % U yield. Strontium was recovered in the intended 0.05 M HNO₃ fraction with an average yield of 70 %. In both trials all the Sr loaded onto the column was accounted for. The remaining 30 % was mostly lost in the wash solutions but for Trial 1 approximately 10 % was lost in the load solution. For both trials 1 and 4 the Th recoveries were consistent with most Th eluted during HCl washing with Trial 1, 79 % and Trial 4, 75 %. Trial 1 recovered 98 % Th and Trial 4, 85 %. Small amounts, <7 % ,were observed in both trials' load and beaker wash solutions.

For trials run with radionuclides of interest in a soil leachate, matrix recoveries were significantly lower but still sufficient for accurate radionuclide determination. Strontium decreased to approximately 50 %, U to approximately 70 % and Pu to approximately 55 %.

With these results, the project successfully achieved the objective regarding the development and implementation of rapid methods for destructive and non-destructive analysis of the radioactivity content of materials on a nuclear site.

4.2. Development and implementation of a novel automatic measurement system to check whether waste packages are safe for disposal or must be treated as radioactive waste

The modified facility for pre-selection of wastes either to radioactive waste repository, or potential free release measurement was installed and commissioned at CIEMAT (Spanish metrology institute) in Madrid. On-site measurements of improved calibration reference materials and radionuclide sources were performed to calibrate the facility detectors and detection efficiencies calculated using two Monte Carlo codes, Penelope and MCNP. Based on the calculations validated by experimental measurements, improved calibration methods were developed allowing activity measurement with relative combined standard uncertainty up to 20% for key radionuclides Cs-137 and Co-60. The facility was also accomplished with neutron detectors for measurement of transuranium elements, such as plutonium isotopes or Cf-252. Real waste packages were measured, such as metal materials (tubes, plates, cables), light materials (plastics, wood), building materials (sand, concrete) and soil.

As part of a research mobility grant (RMG2) studies on the use of Cerium Bromide detectors as an alternative to semiconductor units in the measurement of waste drums have been carried out to determine the efficiencies and decision limits of the detectors setup, as well as to study the viability of the use of spectral indexes to assess the homogeneity of the material inside the drums.

4.2.1. Building of the pre-selection facility

The facility is based on plastic scintillation detectors and low-background concrete shielding with the following main parts:

- Low-background shielding built from low-activity concrete bricks; total weight over 80 tons

- plastic scintillators for pre-selection measurement
- 3 neutron detectors for pre-selection measurement
- 4 HPGe detectors for free release measurement

The overall view and the inner part of the facility with HPGe detectors, plastic scintillators and neutron detectors, and the conveyor are shown in Figure 13.



Figure 13. Overall view of the pre-selection facility (left) and inner part with HPGe detectors, plastic scintillators and neutron detectors, and the conveyor (right).

Low background shielding is made of low-activity concrete bricks, where a concentration of artificial radionuclides is immeasurable and content natural radionuclides is as follows: $a(\text{Ra-226}) \approx 0.6 \text{ Bq/kg}$; $a(\text{Th-228}) \approx 0.3 \text{ Bq/kg}$; $a(\text{K-40}) \approx 6 \text{ Bq/kg}$. Relatively high density of the concrete $\rho \approx 2400 \text{ kg/m}^3$ and dry construction of the whole shielding allow significant reduction of the background inside the measuring chamber.

Dimensions and configuration of the shielding is optimized using Monte Carlo MCNPX code. The chamber's walls thickness is 40 cm, floor thickness is 60 cm and the ceiling thickness is 40 cm. An integral part of the shielding construction is the conveyor, who allows to bring measuring container with wastes from the loading area to the measuring chamber and after measurement to the unloading area. Because of vertically moveable HPGe detectors, one container with a heavy material, or two containers with light material can be measured with total weight of 800 kg.

4.2.2. Facility detectors

The four plastic scintillation detectors NuDET PLASTIC made by NUVIA are based on polystyrene material with a density 1.03 g/cm^3 , refractive index 1.57, softening point 70 - 75 °C, relative light output to anthracene 56%, decay time 2.5 ns wavelength of maximum emission 425 nm. The dimensions of the detector are 1000 x 200 x 100 mm. Detectors are located under and above the container (or containers) with wastes, and on the left and right sides of the container. All four detectors are fixed in the measuring chamber as shown in Figure 14.



Figure 14. NuDET PLASTIC detector for the pre-selection facility.

The three neutron detectors NuDET NEUTRON made by NUVIA consist of a plexiglass light guide on which a ${}^6\text{LiF/ZnS(Ag)}$ detection layer is applied. The thickness of the detection layer is approx. 0.5 mm. A photomultiplier is connected to one side of the light guide to collect scintillation signal. The light guide with the detection layer is wrapped in a reflective and light-tight foil. The whole detector is placed in a 30 mm HDPE moderator to increase detection efficiency for fast neutrons. The sensitivity of the detector is about 470 cps/nv. The dimensions of the detector are 1000 x 500 x 200 mm. All three detectors are fixed in the measuring chamber.

Four HPGe detectors IDM-200V ORTEC are used for free release measurement with nominal resolution 2 keV and nominal relative detection efficiency 50 % for radionuclide Co-60. These maintenance-free detectors constructed for industrial use have a mechanical cooling and are accomplished by lead collimators. Two detectors are located under the measured container and the two others are above the measured container (or containers) with wastes. This measuring geometry allows nuclide-selective measurement with high detection efficiency for gamma-ray radionuclides. All four detectors are fixed in the measuring chamber and vertically moveable.

4.2.3. Waste containers for pre-selection and free release measurements

For pre-selection measurement and free release measurement, three types of measuring containers are used:

- IP1 and IP2 category NUVIA containers with plastic walls, bottom, and lid, strengthened by light steel construction; volume of wastes up to 0.5 m³, max. weight of wastes 500 kg (Figure 15)
- CIEMAT Big-Bag container of robust polypropylene raffia and in an aluminum cage; volume of wastes up to 0.4 m³, max weight of wastes 800 kg, and
- CIEMAT drum 0.2 m³.



Figure 15. IP1 NUVIA measuring container (left) and IP1 NUVIA measuring container (right)

4.2.4. Calibration with reference materials and calibration sources

Improved calibration methods were developed for two typical decommissioning waste materials, metal and concrete, using Monte Carlo (MC) simulations. Four sets of point-like sources type CMI-EG2 with radionuclides Am-241, Cs-137, Co-60 and Eu-152 with metrological traceability to national standards were used for validation of Monte Carlo model for hot-spots calibration, and for experimental determination of minimum detectable activities. Each set contains 12 sources of activities from 30 Bq to 1 MBq. The sources are placed in different positions in the phantoms filled by non-active materials, namely low-activity gravel, empty Petanque balls and plastic balls. Other non-active materials for phantoms are steel Petanque balls without sources and plastic balls. The total efficiencies for plastic scintillation detector were calculated using Monte Carlo codes MCNP and PENELOPE for IP1 category NUVIA container, IP2 category NUVIA container, CIEMAT Big-Bag container and CIEMAT Drum container for each detector, and for all four detectors. The calibration curves were constructed of total efficiency as a function of photon energy. An example is in the Figure 16, where the calibration curve is shown for IP1 container and steel Petanque balls reference material.

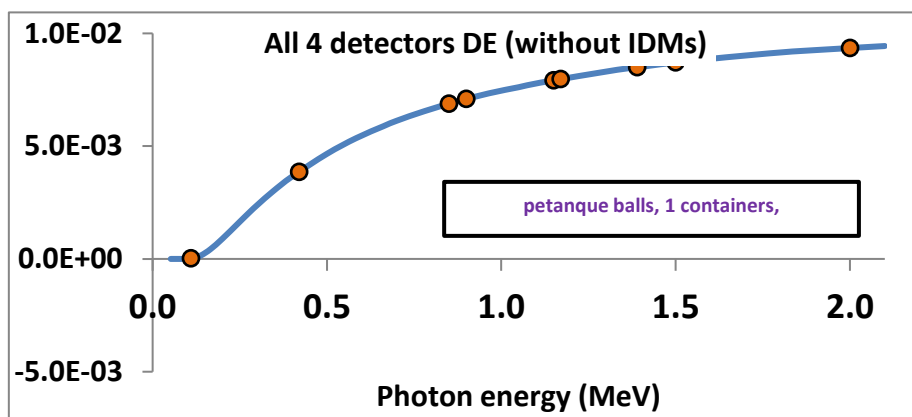


Figure 16. Calibration curve for all four plastic scintillation detectors

Calibration curves calculated using MC codes have been implemented in the pre-selection facility calibration software. MC calibrations detectors were validated using reference materials and standard sources traceable to primary standards for activity of radionuclides and calibration procedures developed with relative combined standard uncertainty less than 20 %. Therefore, the metrological traceability of pre-selection facility has been established.

For measurement geometries, the Monte Carlo calculations of total efficiency were performed and compared to experimentally obtained values by measurement of reference materials and standard sources. The MC model of pre-selection facility has been considered validated, as the difference between measured and calculated values of total efficiency is better than 10 %.

4.2.5. Validation with real waste materials

A set of typical real waste packages was prepared and measured. These are building materials (concrete, sand), metal materials (tubes, pipes, plates, cables), light materials (plastics, wood, glass wool) and soil. The metal materials and light materials were measured in the NUVIA IP1 container, and sand, concrete and soil in the CIEMAT Big-Bag geometry. Representative samples of concrete, sand and soil materials were measured in CIEMAT's laboratories and representative samples of segmented steel tubes and glass wool in CMI's laboratories. The measurement results were used to validate the models and establish pre-selection criteria.

The real wastes measured in NUVIA IP1 container are shown in the Figure 17, including glass wool is in the measuring container and the rest of materials in transport containers.



Figure 17. Real waste materials: pipes, tubes, wood, cables, plastics, glass wool in NUVIA IP1 containers for measurements

4.2.6. Simple example for pre-selection criterion calculation:

- waste material steel tubes, $m = 240$ kg
- radionuclide Cs-137
- container NUVIA IP1
- $\eta_t(662) = 1.1 \times 10^{-2}$ is measuring efficiency for gamma rays energy 662 keV in the energy E range 40 - 2000 keV
- $a_L(\text{Cs-137}) = 300$ Bq/kg is mass activity limit for radionuclide Cs-137 (Czech Atomic Law)
- pre-selection criterion a_{PSC} is selected at 600 Bq/kg
- n is measured net total count rate in the energy range 40 - 2000 keV
- $Y(662, \text{Cs-137}) = 0.85$ is a yield for gamma rays energy 662 keV of radionuclide Cs-137
- pre selection coefficient $PSC = a_{meas} / a_{PSC} < 1$
- The pre-selection criterion can be determined using the formula $n(E) = \eta_t(E) \cdot a(X) \cdot m \cdot Y(E, X)$, where $n(E)$ is net total count rate for gamma-rays energy E in the energy range 40 – 2000 keV.

4.2.7. Free release measurement facility

The free release measurement facility is intended for long-term automated routine measurement on a decommissioning site. Detection efficiency of HPGe detectors for different types of measured wastes and measuring containers was calculated using MCNP and PENELOPE Monte Carlo codes, and validated by traceable reference materials and point-like radionuclide standard sources certified by European metrology institutes. Calibration methods were developed including calibration software allowing calculation of detection efficiency for practically unlimited number of types of wastes and containers. The target relative standard combined uncertainty of 10 % was achieved.

The full-energy peak efficiencies for HPGe detectors were calculated using Monte Carlo codes MCNP and/or PENELOPE for IP1 category NUVIA container, IP2 category NUVIA container, CIEMAT Big-Bag container and CIEMAT Drum container. MC models of HPGe detectors were created and compared, and full-energy peak efficiencies calculated. The total energies were calculated for each HPGe detector, and for all four detectors. The calibration curves were constructed of the efficiency as a function of photon energy. In the Figure 18, the calibration curves are shown for IP1 container with clay balls and gravel reference materials.

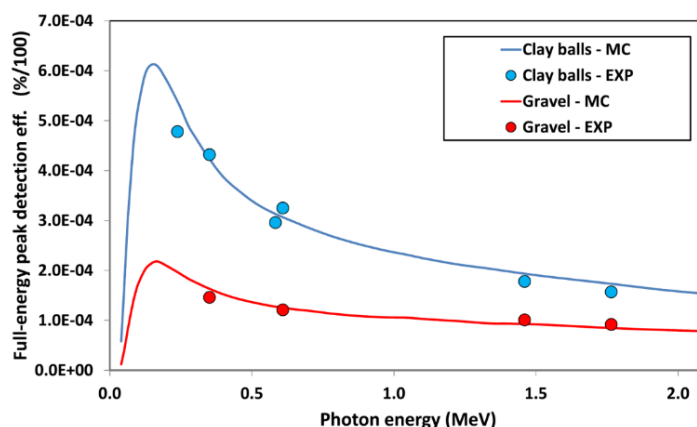


Figure 18. Calibration curves for all four HPGe detectors (clay balls, gravel)

Experimental measurements and the Monte Carlo simulations were carried out for validation of the Free Release Measurement Facility (FRMF) on the CIEMAT's decommissioning site. The validation was performed with five real waste materials from CIEMAT's decommissioning experimental Nuclear Reactor JEM JEN 1. The soil and debris materials are in five Big-Bags of a volume approx. 0.5 m³ each, activity concentrations of the contained radionuclides are of the order of free release levels. The materials contain radionuclides Cs-137, Sr-90/Y-90, Co-60 and traces of actinides, uranium decay series (Ra-226 to Pb-210) and processed uranium (U-238 to Pa-230m). The activity concentrations of different radionuclides were determined to validate the free-release measurement facility prototype for the specific needs of the Waste Management Unit. The validation was carried out with measurements at the FRMF and CIEMAT's gamma spectrometry laboratory, alpha-particle spectrometry laboratory and X-ray fluorescence laboratory. Also, MC model for Big-Bag measuring geometry was created using PENELOPE code.

The comparisons of the results showed very good agreement between radionuclide activity concentrations measured by the free-release facility and those obtained by conventional laboratory radiometric measurements of the same waste materials. The maximum discrepancy in most of the cases was lower than 10 %. Validation using real waste materials confirmed the reliability and applicability of the Free Release Measurement Facility based on 4 HPGe mechanically cooled detectors and low-activity background shielding for safe disposal of radioactive waste from decommissioned nuclear sites.

To summarize, waste pre-selection and free release measurement system has been implemented on a decommissioning site for field trials and upgrades and 'real life' demonstration that it is sufficiently robust for long-term use and meets the strict quality assurance criteria on nuclear sites. The system has been upgraded to include automated density scanning of wastes before measurement and novel software for background reduction to improve sensitivity to meet strict regulatory limits. This upgrade together with traceability to primary activity standards reduces standard uncertainties to better than 20 % for pre-selection of wastes and 10 % for free release measurement. Using special software, the minimum detectable activities have been reduced by 20 to 50 % depending on measured radionuclide and measured waste material. The pre-selection and free release facility has been modified for long-term automated routine measurement on a decommissioning site, including installing, commissioning and validation as well as development of improved traceable calibration methods.

With these results, the project successfully achieved the objective regarding the development and implementation of a novel automatic measurement system to check whether waste packages are safe for disposal or must be treated as radioactive waste.

4.3 Development and implementation of a sophisticated radioactive waste characterisation system, suitable for use as a waste repository acceptance system for very low, low and intermediate level radioactive waste

Globally, significant amount of radioactive waste is generated from a broad range of activities involving the operation and decommissioning of nuclear facilities, activities using radioisotopes in science, industry and medicine, including disused sealed radioactive sources. Such waste needed to be managed in a way that keeps people and the environment safe over long periods. In order to characterise the waste and sentence it into correct waste category, suitable measurement methods were needed that can be performed on materials

properly packed in special waste containers. Measurement methods range from gamma spectrometry (able to perform photon emitters identification and quantification) to passive and active neutron measurements (needed to quantify spontaneous fission and fissile material). Some methods also rely on tomography techniques in order to get information about the distribution of the radionuclides inside each container. Additional dosimetry measurements can be performed on the external part of each container.

4.3.1. Waste Characterisation System

To address these measurement challenges, a fully automatized Waste Characterisation System (WCS) has been previously developed for waste characterisation based on gamma and neutron measurements supported with tomography and dosimetry measurements, and used in this project as a platform to develop and validate methods for waste characterisation. The WCS includes two measurement stations composed of a segmented/tomographic gamma-scanning device and a passive neutron device. Measurement campaigns on both real and simulated waste containers have been carried out by JRC and ENEA and the performance of the systems has been assessed in terms of detection limits, accuracy and measurement time. The entire WCS system is designed to accommodate standard drums of 220 L and 400 L. A schematic view of the system, showing its principal components is given in Figure 19 where the following five individual measurement stations for waste drums of WCS are visible:

- 1 Barcode reading/identification;
- 2 Weight measurement;
- 3 Dose measurement (at contact, and at one metre distance);
- 4 Segmented/tomographic gamma scanning (SGS/TGS);
- 5 Passive/active neutron measurement.

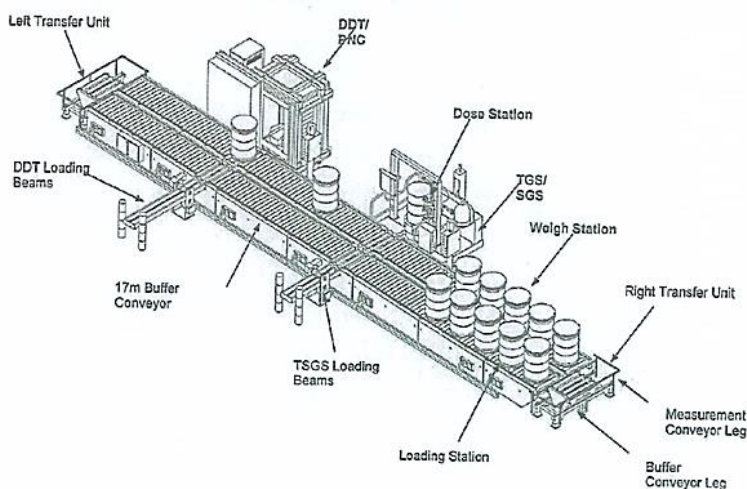


Figure 19. Schematic view of the WCS of the Nuclear Decommissioning Unit of JRC showing main components

The facility is designed for automatic operation of each measurement station and for movement of waste drums between stations. The on and off loading of up to 12 waste drums to the buffer zone on the conveyor is done by means of an overhead crane operated manually. A cyclic procedure like this could see a throughput of 60 standard drums per week or 2000 drums per year.

The gamma measurement station, shown in Figure 20 (left & middle) has the purpose to identify and quantify gamma emitting radionuclides in the waste by implementing both segmented gamma scanning (SGS) and tomographic gamma scanning (TGS), combined with transmission measurements using an external europium (^{152}Eu) source for estimating gamma-ray attenuation in the drum. In the standard SGS mode the drum is measured in 16 horizontal segments with and without the transmission source, while the drum is rotated. In the TGS mode each segment is measured in several voxels by means of both rotation and translation of the drum.



Figure 20. Photos of the of the gamma measurement station (left and middle) and the neutron station (right)

The passive/active neutron measurement station, depicted in Figure 20 (right), has the purpose to quantify the content of the two major actinides uranium and plutonium in the waste. This is done by passive neutron measurement techniques to observe spontaneous fission emitters, and an active measurement using an external pulsed neutron generator to induce fission in fissile isotopes with subsequent detection of the prompt fission neutrons. The combination of neutron measurements of certain fissile isotopes and the determination of the uranium and plutonium isotopic composition allows quantifying with good accuracy the content of uranium and plutonium in the waste item.

4.3.2. Validation of the gamma measurement station

A total of 12 single radionuclide standard point sources, with calibration certificates, were used for WCS validation. Sources were encapsulated in aluminium enclosure for safe operation and prevention of radioactive contamination. Source radionuclides were ^{241}Am , ^{133}Ba , ^{137}Cs , ^{60}Co and ^{152}Eu to cover and define the system operating photon energy range. In addition, a number of simulated waste drums were developed that represent and reflect, as far as possible, the various matrix types encountered in the real wastes at JRC. The simulated waste containers can be filled with various non-active matrix material and have re-entrant tubes for the insertion of reference standard sources or Reference Materials at well-defined locations within non-active material.

In accordance to ISO/IEC 17025:2017 standard and in the method validation context, to characterize the gamma measurement station, a set of measurements on simulated waste (e.g. calibration drum) has been performed. They addressed the following:

- radionuclide to be measured;
- range of detectable and quantifiable total activity;
- its distribution inside a drum;
- position and homogeneity;
- presence of any disturbing or interfering element;
- drum density;
- measuring time;
- repeatability of the measurement.

Gamma measurement station requires an initialization work before to get the system ready to receive a drum for a scan, including an efficiency calibration of the gamma detector and determination of the waste matrix density. Therefore, efficiency calibration has been performed with dedicated drums containing various density wastes in which known radioactive sources are inserted at various positions through vertical channels in the drum. The initialization was performed with a 400 ms measurement in an empty drum at the central vertical axis of the rotatory table. The calibration was performed using four radionuclides: ^{241}Am , ^{133}Ba , ^{137}Cs , and ^{60}Co in technological combustible waste (TCO) to cover the energy range for most of the common radionuclides in nuclear facility waste and the results are given in Figure 21.

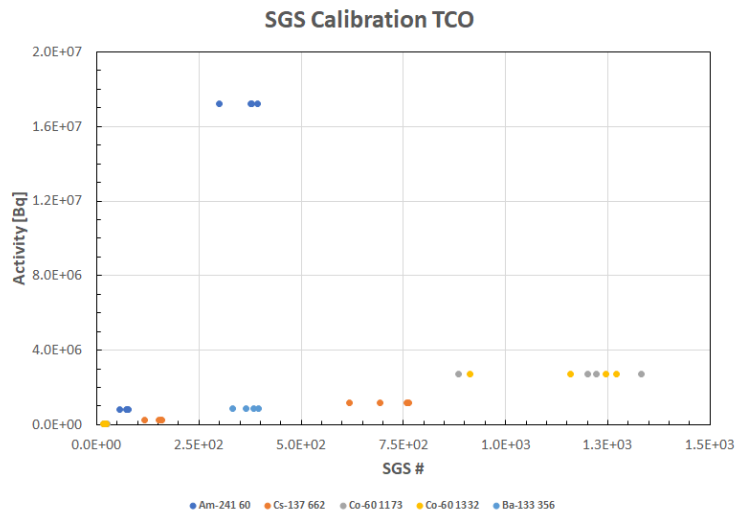


Figure 21. Example of a calibration curve for the SGS mode with four radionuclides in technological combustible waste and their energy of interest

The effect of source position inside a drum was also investigated by performing a series of measurements with ¹³⁷Cs and ⁶⁰Co point sources (encapsulated standard source in an Al enclosure) introduced in each of the 5 different matrixes. The standard 220 L drum has been used with radioactive sources introduced in 7 different channels (A to G) and at three different vertical positions (i.e. top, middle and bottom) on the drum in order to verify the position dependence (Figure 22).

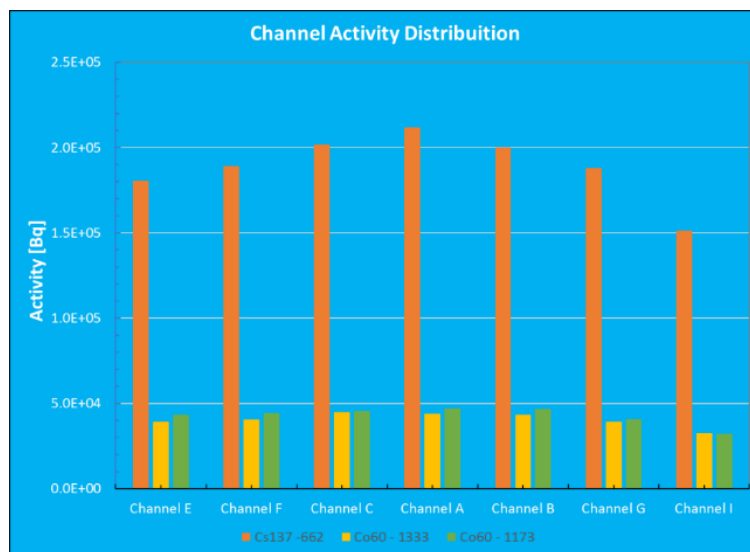


Figure 22. Activity distribution of ¹³⁷Cs and ⁶⁰Co sources in relation to the channel positions

Repetitive measurements were performed on the gamma measurement station in order to assess the repeatability of the results. Ten measurements (1400 ms grab time) were carried out on a TCO drum with a ¹³⁷Cs radioactive source (1.17E06 kBq) in position A3 (i.e. central channel at a middle height of 220 L drum). In the following plot (Figure 23) the TGS results are shown for the central position in a solid blue line while in red the same results from ANTECH TGS Model 3610 (similar setup conditions with a ¹³⁷Cs source in the middle centre position), and a dash red line represent the average activity of the 10 measurements in WCS-Ispra.

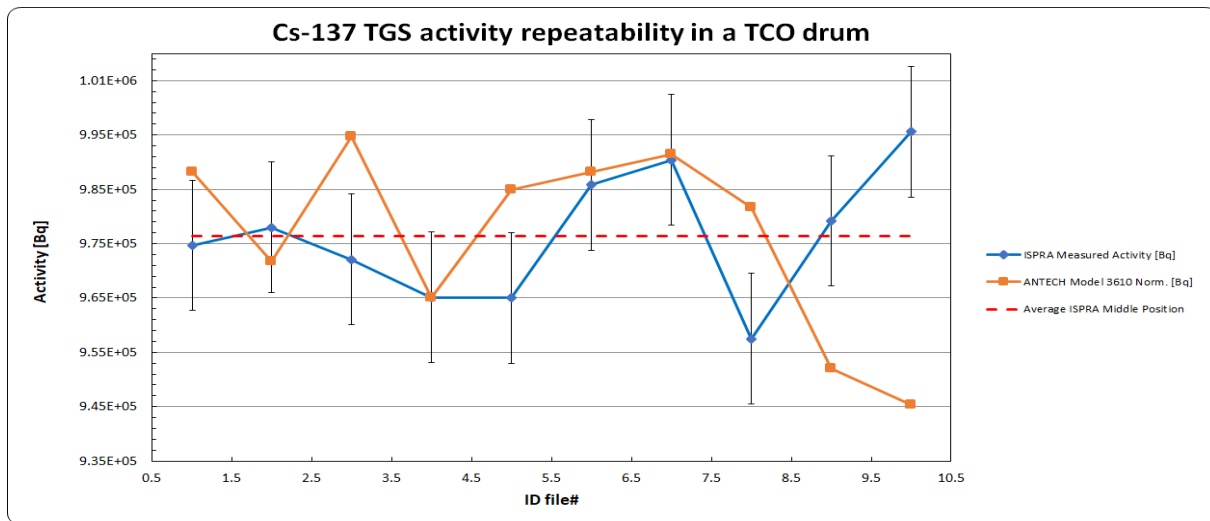


Figure 23. Ten repetitive measurements in TGS mode with a ^{137}Cs radioactive source in position A3 in a TCO matrix drum.

Validation of the gamma measurement station also included analysis of 36 drums containing three types of waste material, which have been selected according to the typology of waste matrix, existing ISOCS measurements and radioactive content according to SGS and TGS calibrations. Those three types of matrix represent the wastes stored in the JRC storage building and include wood, paper and plastic, mixed technological wastes (paper, plastic, chiffonniers or rags, cotton, Tyvek): Technological Waste combustible, **TCO** matrix drum;

1. Glass, fiberglass matrix, glass mixed with paper and plastic: Technological Waste Non-Combustible, **TNC** matrix drum;
2. Demolition wastes, rubbles, stones: Rubbles waste, **RBL** matrix drum.

All the selected drums were produced following to decommissioning and dismantling activities of different buildings at JRC-Ispira site. The drums were selected among those containing ^{241}Am , ^{60}Co and ^{137}Cs as for these radionuclides calibration measurements have been carried out for SGS and TGS. Besides the choice of them has been based on the target value of MDA (minimum detectable activity) evaluated during the characterisation of the WCS. The SGS measurements were performed according the ISOCS measurement time, usually this value is 1h but for very old drums the ISOCS measurements was 3h. Each TGS measurement was performed for 2 h. A comparison between SGS/TGS and ISOCS measurements for the three radionuclides of interest has been performed for 28 waste drums and the results were satisfactory.

4.3.3. Validation of the Passive Neutron Station

Prior to launching the measurements with neutron sources, significant time was spent on the setup and testing of the neutron detection system. The 18 fast neutron detector modules of the passive/active neutron station each has a pre-amplifier/amplifier/discriminator circuitry producing a TTL signal for each detection neutron. The analogue electronics is enclosed in a sealed junction box. Each individual electronic chain is connected to five ^3He detectors was tested to yield the best signal/noise ratio for a common high voltage setting. The final configuration (amplifier gain, discriminator setting) was the best compromise for all modules when operated with a common HV of 1500 volt applied to all ^3He detector tubes. The die-away time of the passive/active neutron station was measured using a ^{252}Cf source placed in the centre of the otherwise empty cavity. Data were acquired with a standard Multi Channel Scalar (MCS), and the measurement points fitted to a single exponential decay as shown in Figure 24.

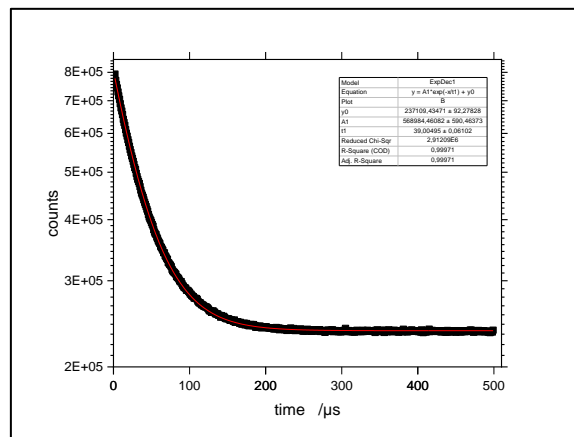


Figure 24. Number of neutron detections as function of time following a neutron detection event at time zero (MCS histogram), including fitting parameters to a single exponential fit.

The least-squares fitting to a single exponential curve shows excellent agreement with the experimental data point. The fitting parameter, the die-away time, equals to $t_1 = 39.00 \pm 0.06 \mu s$. The very good fit indicates a good geometrical design of the fast neutron detection system in the passive/active neutron station.

Pu sources used in the neutron measurement validation campaign were all nuclear Certified Reference Materials certified by the European Central Bureau for Nuclear Measurements (CBNM). The validation procedure included placing the Pu standards at the central position (the position yielding the lowest neutron detection efficiency) for the purpose of verifying that mass determination would indeed provide results reflecting the actually applied Pu mass. The range of Pu mass was chosen to be representative for what could be expected in the waste. In a 2nd series of measurements, a specific Pu standard was placed in various positions in the re-entrant tubes of each simulated drum matrix. The purpose was to verify the ability of the analysis method to determine the correct Pu mass, in conditions where the neutron detection efficiency would vary strongly (with sample position). The accuracy of the mass determination was observed to be in the range of 10-30 % for most waste matrices.

As steps towards the validation of the neutron measurement system, a number of measurement campaigns were carried out using both simulated and real waste drums. Measurements were carried out with the ²⁵²Cf standard source placed in the centre (vertical) plane at the periphery of an empty 220 L drum. The drum was rotated in steps of 15° and the total count rate was measured for at least 20 min in each position. The purpose was to investigate the angular dependence of the combined signal rate in the 18 detector modules. The neutron count rate was recorded in all of the 24 source positions and the result of these measurements is showed in Figure 25.

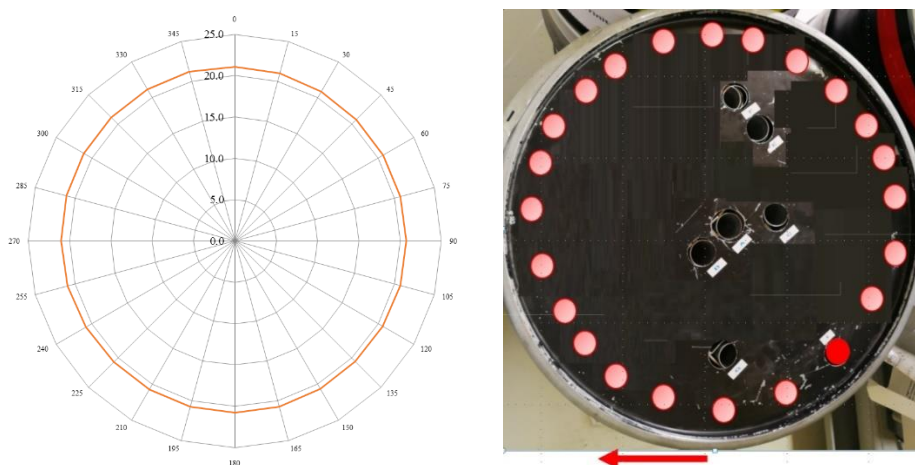


Figure 25. - Angular dependence of detectors response

The measurements performed in air, metal, technological non-combustible, technological combustible, and cement matrices showed that the chosen measurement time (typically 1800 s) could with benefit have been chosen longer, preferably 3600 s in general, and 7200 s for the most hydrogenous matrices (cement, and technological combustible). For the three least-hydrogenous matrices, the assay result agreed within 2-3 standard deviations with the known Pu mass of the standards.

With these results, the project successfully achieved the objective regarding the development and implementation of a sophisticated radioactive waste characterisation system, suitable for use as a waste repository acceptance system for very low, low and intermediate level radioactive waste.

4.4. Development and implementation of (on site) measurement systems and methods for monitoring the condition of radioactive waste repositories, including airborne radioactivity and temperature/strain

During the stages of handling, processing and storing waste arising from nuclear decommissioning it is important to monitor deliberate and unintentional aqueous and gaseous discharges that may contain radioactive isotopes. There was the need to ensure the safety of facility workers, protect the local/regional environment and comply with site permits. These needs are best met with instruments that can perform rapid analysis. Further, the long-term monitoring requirements of decommissioning activities, particularly waste storage, strengthens the case for automated systems that require minimal staff input.

4.4.1. Instrument for measurement of airborne and waterborne radioactivity

A novel instrument was developed for rapid and automated monitoring of radioactive discharges from waste repositories and other nuclear facilities. The instrument (WILMA), developed by LabLogic (LL) is based on a liquid scintillation counting system capable of automatic sampling and measurement of radioactivity (e.g. ^3H , ^{14}C , ^{99}Tc , ^{137}Cs , ^{90}Sr - ^{90}Y , ^{226}Ra , ^{241}Am) in an aqueous stream (Figure 26). An option exists to pair WILMA with a bubbler system to enable in-direct measurement of radioactivity-in-air (e.g. HTO, HT, $^{14}\text{CO}_2$, $^{14}\text{CH}_4$).

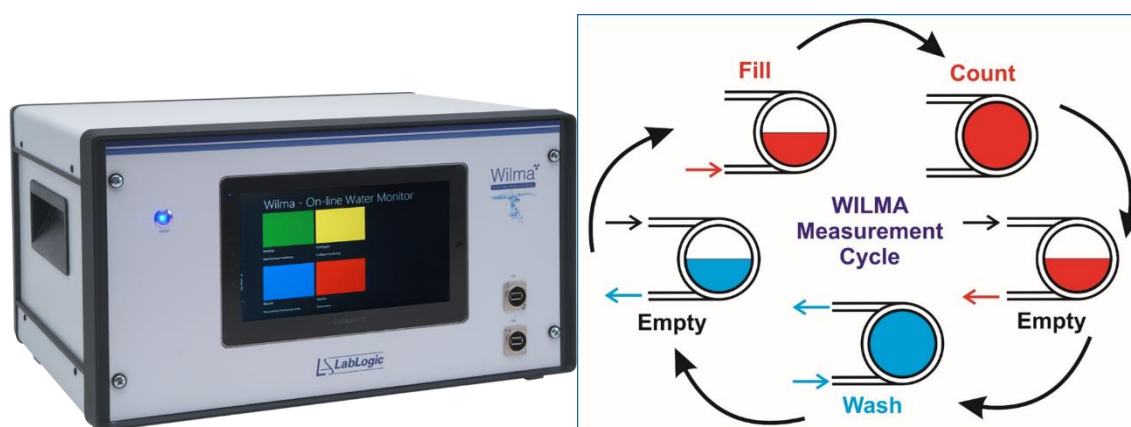


Figure 26. Photo of LabLogic WILMA automated online radioactivity-in-water monitor (left) and schematic view of the LabLogic WILMA measurement cycle (right).

The system was originally designed for unattended on-line monitoring of alpha and beta contamination in drinking water for up to 30 days. Since this initial application, the system has been updated with a rugged and integrated housing, reduced number of fluid connections through use of a manifold design and up-rated pumps and switching valves. The system has been further upgraded to enable sampling from, and refilling of, bubbler bottles. These modifications have been made to allow an SDEC Marc/Hague series bubbler (Figure 27) to be mounted on top of WILMA for indirect monitoring of HTO, HT, $^{14}\text{CO}_2$ and $^{14}\text{CH}_4$ in air. The measurement of HT or $^{14}\text{CH}_4$ is made possible by the inclusion of a catalysed furnace within the Marc/Hague series bubbler. The same system can still be used to monitor for radioactivity in an aqueous stream by amending the protocol to sample from a different port.



Figure 27. SDEC Hague 7000 tritium-in-air bubbler.

The system was tested at a fracking site to investigate its use for monitoring NORM (in particular, ^{226}Ra) in produced and flowback waters. For this, fracking produced/flowback water simulants; high salinity ^{226}Ra standards, were produced for testing the WILMA system. The results were compared with those obtained by a Hidex 300SL TDCR LSC and indicated that the Hidex efficiency values are comparable in magnitude to the WILMA system, albeit higher by around 40 % for the DI water and High+ FS samples and 20 % higher for the High FS samples. This can be attributed to the larger sample volume possible with the static LSC measurement geometry, the different overall counting geometry (2π steradian solid angle coincidence for WILMA vs. 4π steradian solid angle triple and double coincidences for the 300SL) and also through the use of the TDCR technique in order to factor out any contributions from quench. Despite this, the WILMA system still provides more than sufficient counting efficiency to achieve the desired environmental permitting level of 100 Bq L^{-1} with a reduced sample volume and automated sample and cocktail mixing.

Two field trials were also carried out onsite at Culham Centre for Fusion Energy (CCFE). The integrated WILMA-bubbler system was positioned next to the waste drum for measurement as shown in Figure 28. Plastic tubing was used to connect the inlet port of the bubbler to the outlet port of the drum, and vice versa. This configuration produced a closed loop, where 'clean' air was returned to the drum. A pressure gauge was installed in series at the outlet port of the drum to monitor for any drop in pressure, which would be an indication of restricted flow. The bubbler bottles were filled with 150 mL of deionised water. WILMA was configured for 50:50 mixing ratio of sample to scintillant (FlowLogic U).



Figure 28. LabLogic WILMA with integrated bubbler configured for sampling of headspace gas from tritiated soft-waste drum.

A new measurement configuration was successfully developed by NPL and LL and demonstrated through the trials. It was confirmed that rapid measurement of outgassed tritium was possible, with comparable results to traditional lab based LSC measurement.

4.4.2. In-situ monitoring of radiocarbon emissions using laser spectroscopy

Nuclear power plants (NPPs) are constantly monitored to ensure minimum impact on the environment, and most of the radionuclides arising from NPPs are already efficiently measured. However, gaseous radioactive emissions, such as radiocarbon (C-14) and tritium are still challenging to monitor, and a suitable on-line monitoring method is still lacking. Currently used methods are based on technologies requiring labour intensive analysis work and cannot be reasonably converted to automated, field deployable instruments. Therefore,

there is a need for new technologies to ensure more efficient monitoring of radioactive gaseous emissions. To address this measurement challenge, a novel use of laser spectroscopy for in situ detection of radiocarbon at a nuclear facility has been developed by VTT. The measurement is based and represents on a method called cavity ring-down spectroscopy combined with a quantum-cascade laser cavity ringdown IR laser absorption spectrometer for detection of measuring $^{14}\text{CO}_2$ (Figure 29). The system includes an air sampling unit and catalytic furnace to oxidise methane enabling indirect measurement of $^{14}\text{CH}_4$.

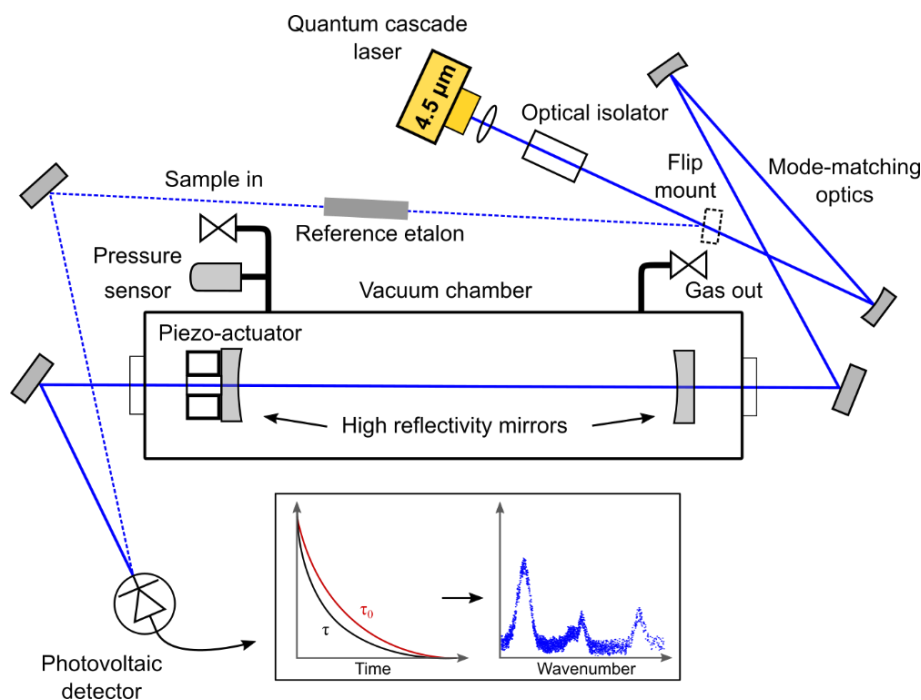


Figure 29. Schematic representation of the instrument for radiocarbon detection. The main path of the QCL laser is shown with the continuous blue line, while the dashed blue line represents the path for laser wavelength calibration through the etalon.

The $^{14}\text{CO}_2$ concentration was measured through the P(20) line at 2209.109 cm^{-1} from the fundamental asymmetric stretching vibration band. With a spectral line intensity of $2.58 \times 10^{-18}\text{ cm}^{-1} / (\text{molecule cm}^{-2})$, the line represents the most distinct spectral feature of the $^{14}\text{CO}_2$, with least overlap with other species, in particular with other CO_2 isotopes. To determine the $^{14}\text{CO}_2$ concentration, a sum of Voigt profiles is fitted to the experimental data, which was first smoothed with a moving average filter. Other absorption lines of $^{12}\text{C}^{16}\text{O}_2$, $^{13}\text{C}^{16}\text{O}_2$, $^{16}\text{O}^{13}\text{C}^{17}\text{O}$ and $^{16}\text{O}^{13}\text{C}^{18}\text{O}$ situated in the vicinity of the $^{14}\text{CO}_2$ line between 2208.9 cm^{-1} and 2209.18 cm^{-1} are included in the fitting model. A gas sample with a known $^{14}\text{C}/\text{C}_{\text{tot}}$ ratio of 1.01 ppb prepared earlier was used to characterise the system. The measured concentration by cavity ring-down spectroscopy (CRDS) at 10.10 mbar pressure was $^{14}\text{C}/\text{C}_{\text{tot}} = 1.0 \pm 0.2\text{ ppb}$. The main source of the uncertainty was instrumental noise, resulting from all the components being in close proximity to each other causing interferences. For instance, mechanical vibrations and electromagnetic noise from the pump could not be completely isolated from the other components in the assembly.

The atmospheric CO_2 concentration is about 400 ppm and similar levels are measured in NPP stacks. To reach the highest sensitivity in radiocarbon detection, CO_2 needs to be first captured and purified from the sample air, as the targeted $^{14}\text{CO}_2$ concentrations are too low to be measured directly at the atmospheric CO_2 concentration. Therefore, an on-line automated sample-processing unit was coupled to the CRDS instrument. A solid amine type sorbent ion-exchange resin was used as the trapping material. The resin efficiently and selectively adsorbs CO_2 from air at room temperature and the CO_2 desorbs by heating the resin to a temperature of $50 - 100\text{ }^\circ\text{C}$. Two parallel CO_2 traps were made of aluminium cylinders and filled with the resin. The traps were heated resistively, while active cooling was achieved with heat sinks and fans. The traps were connected in parallel as shown in Figure 30 to trap sample air alternately. In this configuration, one trap can release trapped CO_2 to the spectroscopy unit and cool down, while the other trap is collecting CO_2 for the next measurement.

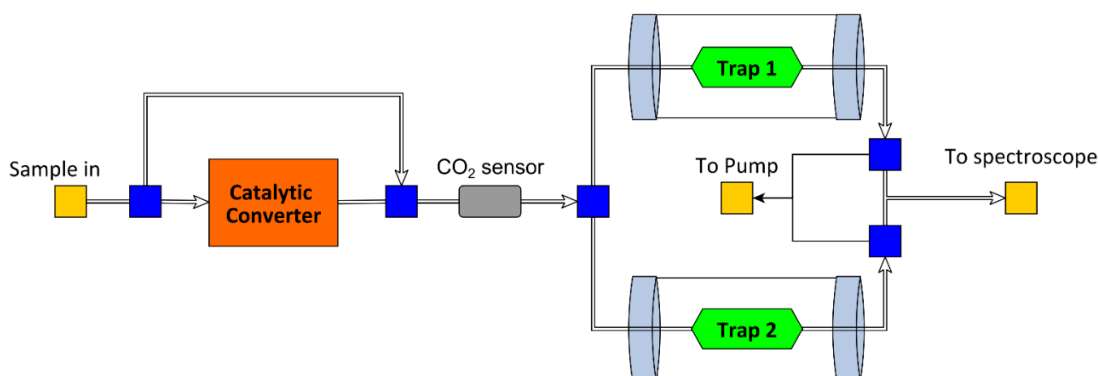


Figure 30. Sample-processing unit. The sample flow direction is controlled by solenoid valves represented by the blue squares.

The main source of uncertainty in the ^{14}C measurement is the $^{14}\text{CO}_2$ line fitting, which mainly depends on the uncertainty in the determination of the ring-down times and on the drifts in the laser wavelength, resulting from instrumental noise. The same factors affected also the line fitting in the CO_2 cavity concentration measurement, but this measurement had much smaller effect on the total uncertainty, as a stronger absorption line was probed. Other sources of uncertainty were considered small in comparison to the uncertainties in the spectral line fits. The detection limit of the system was $^{14}\text{C}/\text{C}_{\text{tot}} = 0.25$ ppb, corresponding to activity of about 10 Bq/m^3 in air with a CO_2 concentration of 400 ppm.

The developed prototype instrument was used to monitor in situ the ^{14}C emissions from the Loviisa nuclear power plant in Finland. The measurement campaign took place in September – October 2019, during which continuous automated monitoring of ^{14}C emissions was demonstrated for the first time. Radiocarbon is currently measured in a radiochemistry laboratory with LSC after collection of the sample to a molecular sieve from the stack gas flow. The sample collection time to the molecular sieves ranges from a few days to two weeks. Few days of trapping is the minimum requirement to collect sufficient amount of CO_2 for the subsequent LSC analysis. The time resolution for this method is poor, as the acquired radiocarbon activity is the average activity of the collection time: a few days at best. Short time variations are thus undetectable with the current method.

In Loviisa NPP, a fraction of the air exiting through the stack is collected via separate monitoring lines for each reactor to be analysed for radiocarbon, tritium, iodine, noble gases and other radioactive content. The airflow through the monitoring lines is 30 – 70 l/min and the residual airflow is returned to the stack exhaust after analysis. The operators collect sample for the conventional radiocarbon analysis with molecular sieves situated on the monitoring lines. For the radiocarbon analysis with CRDS, we connected our sample inlet to the monitoring line before the molecular sieve and returned the residual airflow back to the line downstream of the sieve. The airflow during trapping through the sample-processing unit with the catalytic converter was 0.7 l/min for the total radiocarbon analysis and 1.0 l/min for the detection of radiocarbon in carbon dioxide when the converter was bypassed. Trapping time of 45 minutes was used for a single radiocarbon sample in the CRDS measurement to ensure sufficient CO_2 trapping even if the sample air composition varies. Still the CRDS measurement was remarkably faster than the few days duration with the conventional molecular sieve–LSC method.

Two example spectra recorded at the plant are shown in the Figure 31, where a clear difference in the $^{14}\text{CO}_2$ peak intensities is observed between two measurements from reactor 1(LO1) on September 25th in (a) and reactor 2 (LO2) on September 26th in (b). From the line fitting and the determination of C_{crds} , C_{air} and C_p , the radiocarbon activity concentrations for the two spectra were 45 Bq/m^3 ($^{14}\text{C}/\text{C}_{\text{tot}} = 1.1 \pm 0.2$ ppb) and 246 Bq/m^3 ($^{14}\text{C}/\text{C}_{\text{tot}} = 6.0 \pm 0.3$ ppb) in (a) and (b), respectively. The amount of N_2O could be determined using the line at 2209.085 cm^{-1} and the concentration was 2.2 ppm in (a) and 1.9 ppm in (b). The two spectra were measured at cavity pressure of 7.5 mbar. The purified CO_2 concentrations in these measurements were 90 % and 76 % for (a) and (b), respectively. The lower CO_2 purity in (b) with higher ^{14}C concentration is assumed to be in connection with the fact that most of the ^{14}C is in the form of methane and other hydrocarbons. Catalytic combustion of hydrocarbons produces water, which co-adsorbs with carbon dioxide to the resin and reduces

its capacity for CO₂ absorption. With higher C14 concentration, higher amount of hydrocarbons is expected, resulting in increased water content in the sample gas flow through the traps.

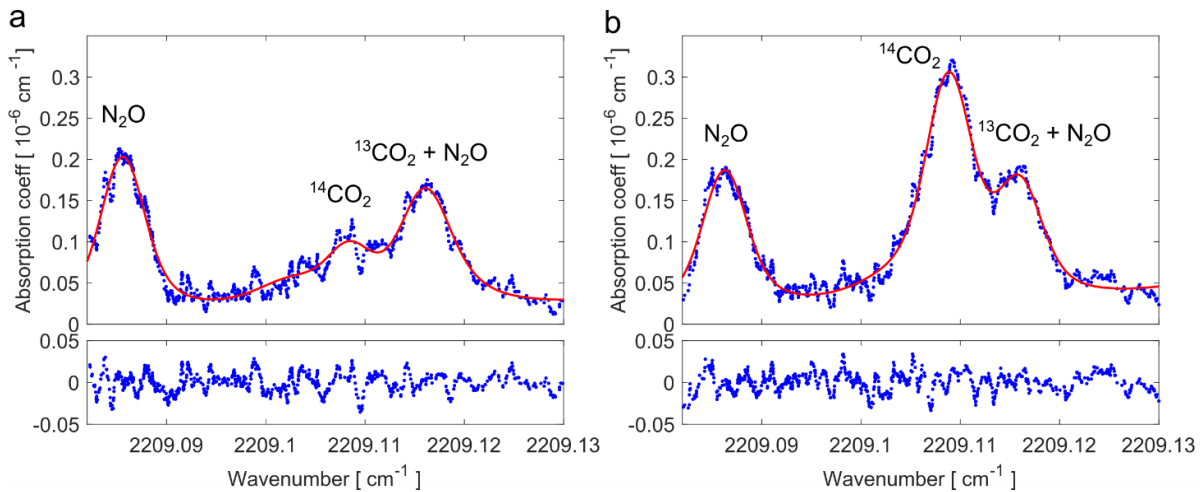


Figure 31. Two absorption spectra recorded from the nuclear power plant stack, recorded on September 25th (a) and 26th (b). The ring-down data, shown in blue, is smoothed with a moving average filter. The red lines represent the fitted sum of Voigt profiles and the corresponding residuals are shown below. A clear difference in the intensity of the ¹⁴CO₂ peak at 2209.109 cm⁻¹ is visible. In (a) the concentration of C14 was 1.1 ppb while in (b) it was 6.0 ppb. The N₂O line at 2209.085 cm⁻¹ was used as an anchoring point for the wavenumber scale.

The presented CRDS method proved to be very suitable for the monitoring of fugitive radiocarbon emissions, with an unprecedented temporal resolution. It allows measuring fluctuations of the radiocarbon activity concentrations, which could not be captured with currently available methods. The CRDS connected with the presented sample-processing unit allows determination of the amount of radiocarbon in different molecular forms. The time resolution of the instrument can still be enhanced by reducing the CRDS cavity volume, so that less CO₂ is required and shorter trapping time is needed. At best, the time interval between measurements can be brought down to few minutes, which can provide more detailed information on radiocarbon discharges within a nuclear facility. The testing and validation work demonstrates the feasibility of this technique for onsite measuring of ¹⁴C and other gaseous radionuclides.

4.4.3. Validation of procedures for metrological characterisation of Distributed Strain and Temperature Sensing (DSTS) systems

Radioactive waste repositories (deep geological or surface, dependant on the waste category) and power plants required an important lifetime of the sensors, maintenance-free, to cover the monitoring period of several decades. The use of optical fibres as distributed sensor is promising because it provides distributed measurements performed at the overall structure scale instead of being limited to local effects. Techniques based on spatially distributed measurements of temperature and strain by optical fibre have been used for several years for the monitoring of road infrastructures (bridges, tunnels) or hydraulic ones (dams, dikes) over long distances (tens of kilometres). As an example, the monitoring of temperature profiles by means of optical fibres represents a highly efficient way to perform leakage detection along dikes or embankments.

The development of radiation resistant optical fibres enables now the implementation of such optical fibre sensors in nuclear environment. As new technologies, such distributed measurement systems are not yet fully concerned by standards which would frame their implementation conditions. In particular, in front of the commercial offer already available, the choice of the most appropriate device is not obvious for the user as regards its application. The lack of standards which would frame the characterization of such systems doesn't enable to compare them from relevant metrological characteristics. Only standardized experimental protocols dedicated to evaluate a set of well-defined metrological characteristics associated to distributed measurement systems would provide a mean to shed-light the user to take the final decision with respect the purchase of the most appropriate system suitable to the requirements as regards to the aimed application. The Raman distributed temperature sensing (DTS) and Brillouin distributed strain and temperature sensing (DSTS)

technologies are currently under evaluation by the nuclear and hydraulic industries since they may bring an alternative to classical measurement techniques. The reliability of the DTS and DSTS measurements, as well as their traceability to the temperature standards, must be ensured throughout the entire period of monitoring, typically over a few tens of years. To achieve this goal, the metrological performances (sensitivity, resolution, stability...) and characteristics of the DTS and DSTS devices, as well as the practical aspects on their implementation and calibration on site must be evaluated step by step.

For characterisation of DTS and DSTS devices, two thermal enclosures have been designed by LNE in partnership with EDF and ANDRA. The first one is dedicated to the interrogator while the second one is devoted to the sensing optical fibre. By the mean of heat exchangers with circulating thermalized water, each enclosure can be separately adjusted at different temperature levels within the range 3 °C – 60 °C. An arrangement of fans into the enclosures enables to ensure the temperature homogeneity into the enclosures within 0.1 °C. Figure 32 illustrates a typical experimental arrangement for the thermal characterization of a Raman-DTS system.

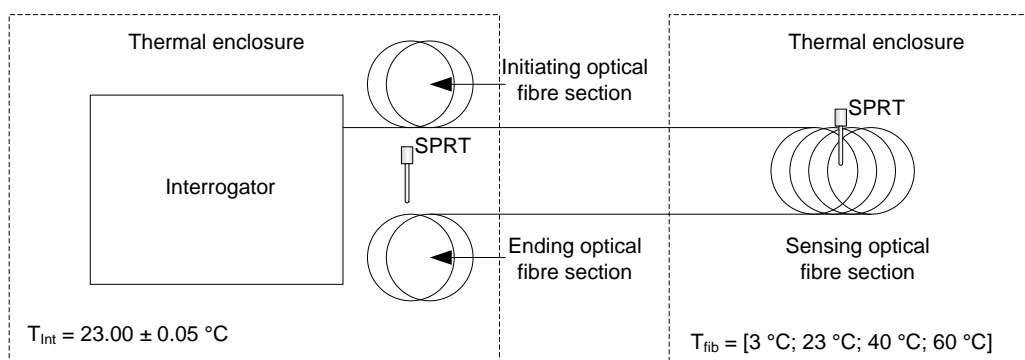


Figure 32. Typical experimental arrangement of the DTS-Raman interrogator and the sensing optical fibre, each of them placed into their dedicated temperature-controlled enclosure.

Two initiating and ending optical fibre wounds (with a length of 500 m each) are positioned within the same enclosure of the interrogator. Such optical fibre sections located at the two ends of the measurement line enables to adjust the interrogator internal temperature calibration parameters, as it is described into the following paragraphs. A standard platinum resistance thermometer (SPRT), periodically checked into a molten ice bath at 0 °C, is placed in each enclosure to enable the direct temperature traceability to the SI.

The main measuring optical fibre has a length of 4, 9, or 19 km. Two initiating optical fibres with a length of 500 m each are welded on both ends of the main spool by the mean of fusion splices (local losses less than 0.02 dB). Then, the full optical fibre circuit have a length of 5, 10, or 20 km, in accordance with the maximum measurement range of the tested interrogator. The reference fibre is periodically checked (ideally, before to start the characterization process) with a reflectometer in order to detect any located deviation of the attenuation coefficient along the fibre length which could generate unexpected measurement artefacts/bias.

For pre-calibration of the Raman-DSTS systems, the interrogator was calibrated at a reference temperature of 23 °C (close to the room temperature). Once a temperature trace is measured, the slope coefficient was adjusted. The alignment of the temperature signals measured over the two ending fibre sections (arranged within the interrogator thermal enclosure) enabled to adjust the slope coefficient to its appropriate value. Then, temperature offset coefficient was set adjusted to centre the temperature signal from the first ending fibre section on the temperature value measured. Figure 33a illustrates the effect of the slope and offset corrections on a temperature trace, while Figure 33b shows the result of such a pre-calibration on an interrogator.

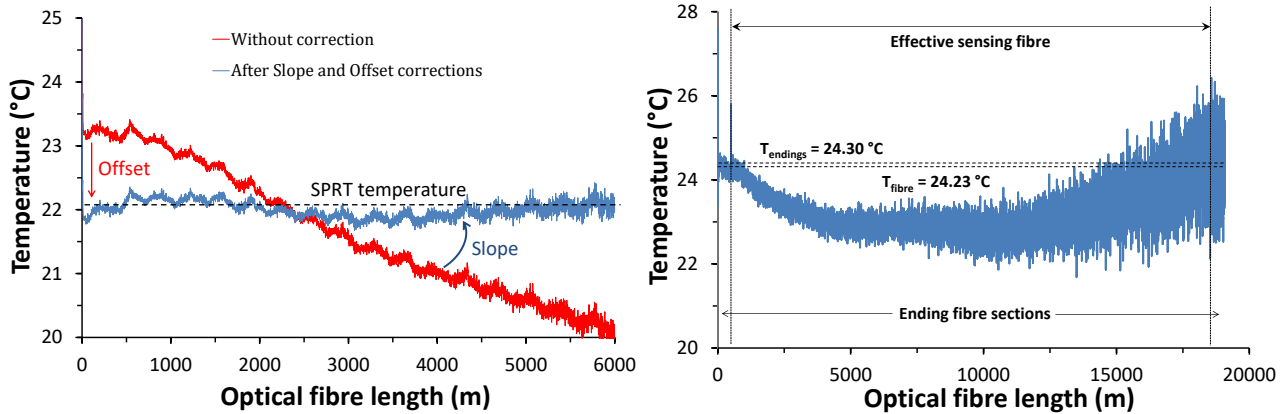


Figure 33. a) Example of a temperature trace corrected by the slope and offset coefficients; b) Temperature trace after the pre-calibration of an interrogator.

Furthermore, a measurement of the trueness error was performed which is defined as the deviation of the fibre temperature measured with the SPRT and the effective temperature measured by the DTS-Raman interrogator. The interrogator was thermally stabilized at the normal room temperature (23 °C), and the optical fibre was successively stabilized at least at four temperature levels within the range 0 – 60 °C (3 °C, 23 °C, 40 °C, and 60 °C in the current set of measurements). The temperature trace (Temperature Vs. fibre length) was affected by noise as seen in Figure 34.

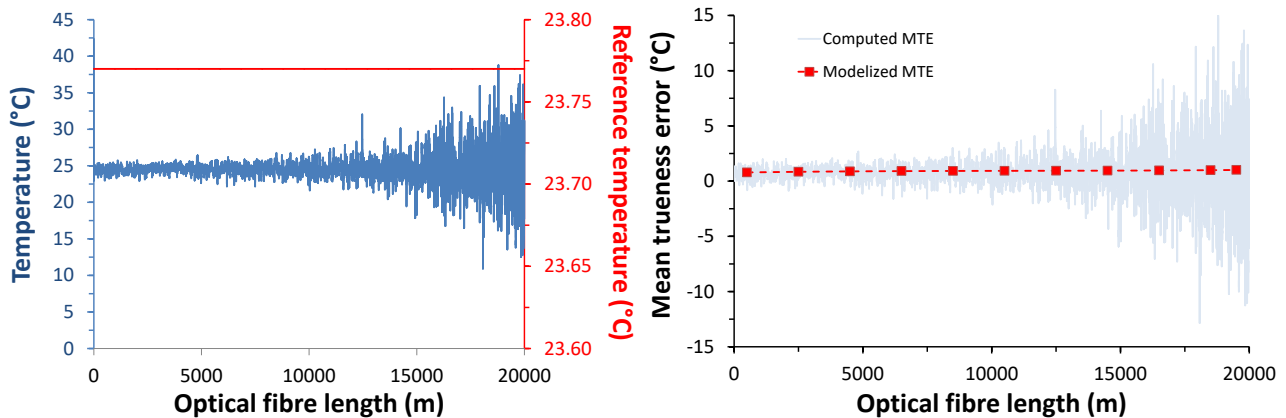


Figure 34. Temperature trace measured with a Raman-DTS system and sensing optical fibre thermally stabilized at ~23 °C, SPRT temperature signal is superimposed (left), and, mean trueness error computed and superimposed to the modelized signal by 3rd order polynomial regression (right)

A Raman-DTS system generally proposes to select an integration time for performing the measurement. It is possible to perform a short-time measurement (30 s or 60 s for instance) or a long-time acquisition (up to 3600s). Typically, the system requires approx. ten seconds to perform a full scan of the optical fibre. A 30 s integration time significates that the interrogator will perform to three successive measurements and will provide a temperature trace which is the averaged signal computed from the three full scans of the line. Thus, the more the integration time is higher, the more the temperature trace is smoothed (and the signal-to-noise ratio appears optimized). This setup has a direct influence on the spatial dispersion (and temporal repeatability by the way). It might be noted that some of the datasheets provided by manufacturers to describe the capabilities of their interrogators are given for measurement performed at the highest integration times, which are consequently often very optimistic. Spatial dispersion measurement can be performed on a given interrogator for different integration times. Typical results obtained with an optical fibre stabilized at 23 °C are presented in the Figure 35.

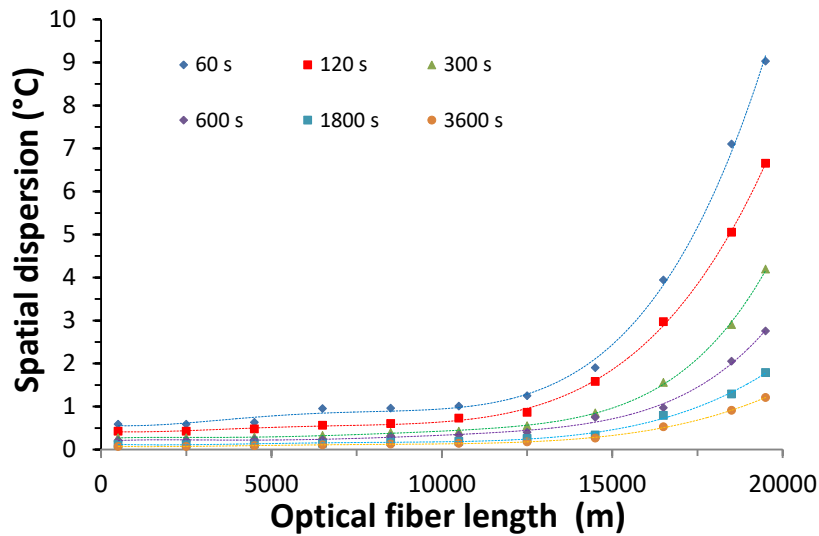


Figure 35. Spatial dispersion measured at different integration times with an optical fibre thermally stabilized at 23 °C.

A key project objective was to validate the performance of a cartridge prototype, and to demonstrate its traceability to the temperature standards, in order to finally validate its exploitation on site. Such cartridge has to generate a uniform, stable and well-known temperature over a cable portion whose length corresponds to the spatial resolution of a DTS unit under test, in order to verify the performance claimed by the manufacturer. The cartridge designed by LNE relies on the combination and adaptation of various sub-elements to control and measure the temperature and its distribution over a length of optical fibre to monitor its long-term drift and allow its use in various environments. Sensing fibre is inserted into a central tube (Figure 36, "2"). The central tube is positioned in the middle of a copper conductive block which is temperature controlled. The conductive block is equipped with heating elements connected to an external temperature controller by means of a waterproof connector (Figure 36, "4"). The block is equipped with several temperature probe distributed so in order to evaluate its thermal stability and homogeneity. The thermal cartridge is 1.2-meter-long, maintaining a fibre cable section of 1 meter long at a uniform temperature on the time scale of the DTS measurement.

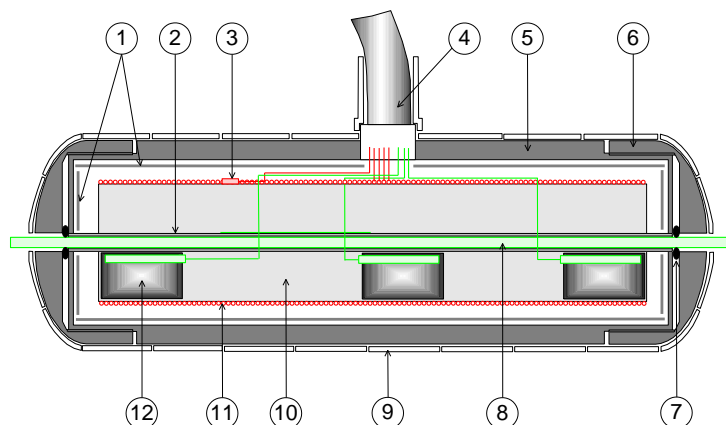


Figure 36. Thermal cartridge: 1. Radiation shields - 2. Central tube – 3. Control probe – 4. Multi-conductor shielded cables and waterproof connector - 5. Outer casing – 6. Waterproof caps – 7. O-ring - 8. Fibre cable - 9. Geotextile - 10. Copper conductive block – 11. Heating element – 12. Mini crucible containing re-usable eutectic alloys and associated temperature sensor.

A thermal cycle of the cartridge from room temperature to 88 °C is shown in Figure 37 together with the temperature measured along time by one of the three temperature sensors inserted into its associated mini-cell. It has to be noticed that all five temperature sensors and their associated indicator were calibrated to ensure traceability to the International Temperature Scale (ITS-90) prior to the cartridge assemble and all three mini-crucibles containing the three eutectic alloys were characterized in terms of temperature and repeatability of the melting point temperature.

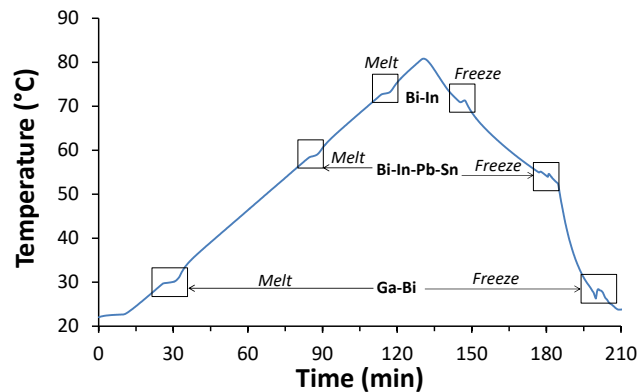


Figure 37. Typical PRT calibration cycle with a 3 fixed-point cell.

After assembly, the cartridge was tested in a temperature-controlled environment (between 20 °C and 23°C). The tests were carried out in air then by immersion of the cartridge in sand to simulate a typical on-site environment. The melting temperature of the mini-cells showed good consistency, within 0.04 °C, with the temperature as observed before assembly of the cartridge, validating all temperature measurements. The temperature stability and homogeneity of the cartridge was then measured at 23 °C, 43 °C, and 80 °C. The temperature homogeneity was measured by altering the position of a temperature sensor placed in the central tube of the cartridge. Results showed a temperature stability of up to 0.07°C (standard deviation) and a temperature homogeneity of up to ± 0.9 °C over 1 meter at 80 °C.

A field experiment was also carried out to test the methodologies developed in the laboratory fulfil the requirements for onsite application identified by EDF and ANDRA. In this field installation, an optical fibre passed over the thermal cartridge placed inside the floor of a tunnel in the underground laboratory of Meuse/Haute Marne. As illustrated by Figure 38, cartridge was subsequently immersed in the concrete structure of the tunnel. Cartridge was cycled between ambient temperature and 80 °C several months after its installation. Operations were controlled by the operator 400 km away from the tunnel. The cartridge demonstrated good general operation. Again, the observed melting temperatures showed excellent consistency, within 0.03 °C, with those previously observed in ideal laboratory conditions. The temperature of the cartridge was stabilized at three temperatures above ambient temperature.

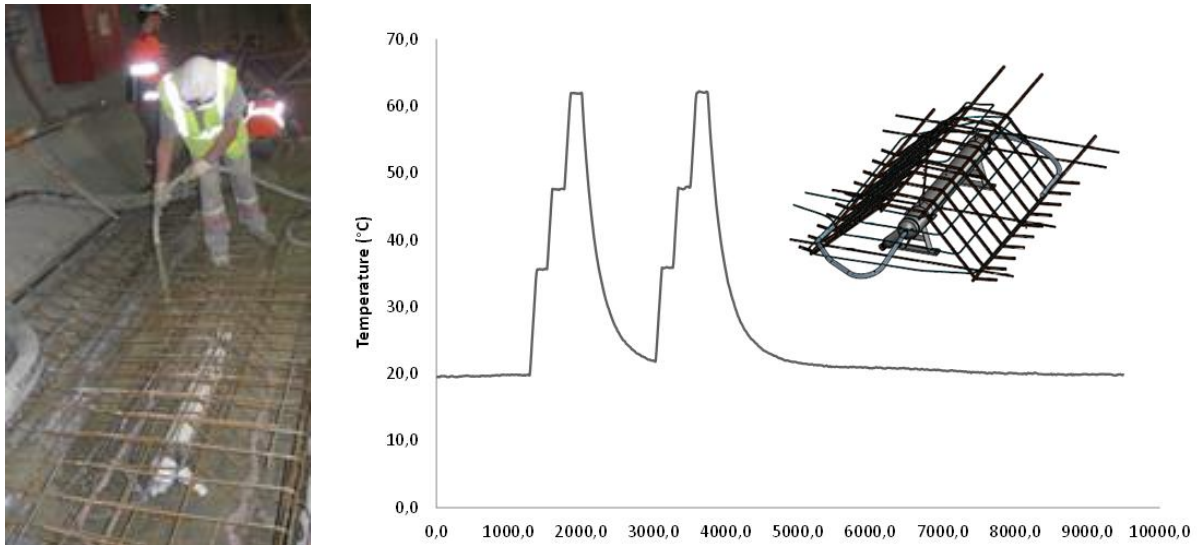


Figure 38. Integration of the cartridge within the floor gallery structure (left), and on-line thermal cycles performed on the cartridge for the in-situ calibration of the sensing optical fibre (right).

As previously observed, a large deviation was found between the actual temperature of the cartridge and the temperature measured with the DTS unit. At specified temperatures however, the observed deviation was found constant with time. With the deployment of DTS instrumentation in the nuclear field, the quality of data has to be certified. There is therefore a strong need for a standardized vocabulary able to clearly describe the characteristics of such novel measurement technologies, for metrological studies of such instrumentations, and for the development of on-field calibration systems.

With these results, the project successfully achieved the objective regarding the development and implementation of onsite measurement systems and methods for monitoring the condition of radioactive waste repositories, including airborne radioactivity and temperature/strain measurements.

5. Impact

As part of disseminating the project results, a dedicated blog was set up and regularly updated to provide up to date results and information. A Stakeholder Committee was established to participate and gave feedback and steered the work of the consortium. Within the course of the project five open access peer-reviewed articles have been published in relevant scientific journals and four more have been submitted. The main results and outcomes of the project were presented at 27 international and national conferences and five training courses have been provided to the project consortium, stakeholders and university students.

Impact on industrial and other user communities

The main impact of this project on the nuclear decommissioning community was through the delivery of methods, instrumentation and procedures developed to ensure that radioactive waste is accurately characterised and safely managed. More specifically, the portable instrumentation prototypes and procedures developed, tested and validated for in-situ measurement of gamma- and alpha-emitting radionuclides could be adopted for use by decommissioning personnel on nuclear sites to screen and measure radioactive contamination and plan decommissioning activities. The semi-automated micro-fluidic system for radiochemical separation has the potential for significant cost and time saving for the determination of difficult to measure radionuclides in radioactive waste and materials originating from nuclear licence sites. The set-ups for laser-spectroscopy measurement of radiocarbon and automated liquid-scintillation counting of airborne-radioactivity had routes to the market through the instrumentation companies that were partners during the project, but also with early adopters likely to be nuclear power plants, decommissioning sites and low-level waste repositories in the UK, Finland, France and other EU countries.

The project also involved testing, calibration and validation of two major facilities: the waste-package sentencing system and the waste-repository measurement system. The immediate impact from these facilities will be on accurate, traceable, regulatory-compliant assessments of radioactive waste for the nuclear sites

where the facilities are located, but also the use of these facilities to disseminate best practice and traceability to all nuclear sites operating waste package measurement systems.

Impact on the metrology and scientific communities

To address the measurement challenges in decommissioning (different radionuclides, different materials & activity levels), the project activities resulted in the development of novel advanced methods for radioactivity measurements, contributing to the establishment of harmonised, international measurement infrastructure to support nuclear decommissioning. Highly efficient procedures have been developed for the analysis of radionuclides of significant relevance for nuclear decommissioning and radioactive waste characterisation such as actinides, ^{90}Sr , ^{41}Ca , ^3H , ^{14}C with potential application in other scientific areas, i.e. environmental monitoring.

Impact on relevant standards

The project will have impact on standards being developed by the International Organisation for Standardisation (ISO). ISO standards are of essential importance for laboratories and measurement scientists throughout the nuclear industry and have been adopted in many countries as national standards. The technical findings have been fed back for incorporation in standards under development and new work items covering topics such as the use of sensor networks at ISO/TC85/SC2/WG17 and improved radioanalytical methods for radioactivity measurements ISO/TC147/SC3. The work contributes to national good practice guides, such as the proposed UK Nuclear Industry Code of Practice for site characterisation.

The project partners have also contributed to the preparation of international standards in three IEC/ISO committees: i) IEC/TC86/SC86C/WG2 Fibre optic sensors, ii) ISO/TC85/SC2/WG14 Air control and monitoring, iii) ISO/TC147/SC3/WG14,15&16 Radioactivity measurements.

Longer-term economic, social and environmental impacts

The main long-term impact on the nuclear industry would be a reduction in the cost of disposal of waste. The cost of disposal depends on the radioactivity content of the material; in the UK, 'non-radioactive' waste costs about £200 ton⁻¹ to dispose, very low-level waste is about £750/ton and low-level waste about £3000 m⁻³. Estimates of the cost of disposal of higher activity waste depend on the financial model used but vary from £12000 m⁻³ for ILW to £300000 m⁻³ for HLW (or higher). Traceability to national standards and better understanding of the measurement uncertainties gives improved confidence in the results to the regulators (and also the members of the public); this enables the industry to recycle or re-use more of the waste that is produced, and to use lower category waste disposal options (current practice is to be overly conservative, which increases costs with no benefit to the environment). It is difficult to quantify the potential savings, but even a marginal improvement in dealing with the wastes will result in significant costs savings (the UK alone estimates that decommissioning legacy nuclear sites will produce 2,840,000 m⁻³ very low-level waste, 1,370,000 m⁻³ of low level waste and 286,000 m⁻³ of ILW). In addition, improved traceability will reduce the need for re-work to investigate apparent discrepancies in measurements. The links to the industry-independent international measurement system will improve public trust and confidence that radioactive waste is being disposed of safely.

Furthermore, the project results will have impact on distributed strain and temperature sensors based on optical fibres, which have many applications in structural health monitoring. DTS and DSTS sensors have potential applications monitoring a wide range of engineering structures: ageing of rail infrastructures, mechanical and hydraulic behaviour of dams and dykes, breakage and leakage detection systems of gas, water and oil pipe-lines (the nuclear industrial sector is also interested by these technologies for monitoring the concrete structures of power plants). Such optoelectronic devices will also play a more prominent role in a smart city framework with detection of frozen roads, soil parameters analyses in agronomy, or monitoring of telecommunication/high voltage cables.

Novel radiochemical separation techniques have potential for impact in nuclear medicine, where similar technologies are being used for purifying radionuclides for use in radiopharmaceuticals for diagnostic scans and cancer therapy.

The technologies for remote measurement of alpha emitters and for imaging the location of gamma emitters have potential applications in the defence sector, particularly for use by first responders following the detonation of a so-called 'dirty bomb'.

The technology developed for monitoring ^3H and ^{14}C at repositories may easily be adapted for use at other nuclear facilities, for example, for stack monitoring for radionuclide production facilities or for radiation protection on operating nuclear power plants, fusion research centres or defence facilities.

6. List of publications

G. Failleau, O. Beaumont, R. Razouk, S. Delepine-Lesoille, M. Landolt, B. Courthial, J.M. Hénault, F. Martinot, B. Hay. A metrological comparison of Raman-distributed temperature sensors. *Measurement* 116, 18-24 (2018). <http://dx.doi.org/10.1016/j.measurement.2017.10.041>

E. Braysher, B. Russell, S. Woods, M. García-Miranda, P. Ivanov, B. Bouchard, D. Read. Complete dissolution of solid matrices using automated borate fusion in support of nuclear decommissioning and production of reference materials. *J. Radioanal. Nucl. Chem.* 321(1), 183-196 (2019). <https://doi.org/10.1007/s10967-019-06572-z>

G. Genoud, J. Lehmuskoski, S. Bell, V. Palonen, M. Oinonen, M.-L. Koskinen-Soivi, M. Reinikainen. Laser Spectroscopy for Monitoring of Radiocarbon in Atmospheric Samples. *Anal. Chem.* 91, 12315–12320 (2019). <https://doi.org/10.1021/acs.analchem.9b02496>

T. Kerst and J. Toivonen. Dynamic Enhancement of Nitric Oxide Radioluminescence with Nitrogen Purge. *Sci Rep* 9, 13884 (2019). <https://doi.org/10.1038/s41598-019-50396-6>

F.S. Krasniqi, T. Kerst, M. Leino, J.-T. Eisheh, H. Toivonen A. Röttger J. Toivonen. Standoff UV-C imaging of alpha particle emitters. *Nuclear Instruments and Methods in Physics A.* 987, 164821 (2021). <https://doi.org/10.1016/j.nima.2020.164821>

This list is also available here: <https://www.euramet.org/repository/research-publications-repository-link/>

7. Contact details

Project coordinator: Peter Ivanov
National Physical Laboratory, Hampton Rd, TW11 0LW Teddington, UK
Email: peter.ivanov@npl.co.uk
Phone: +44 (0)20 8943 8598
